


# Molluscan Dorsal–Ventral Patterning Relying on BMP2/4 and Chordin Provides Insights into Spiralian Development and Evolution

Sujian Tan,<sup>†,1,2,3</sup> Pin Huan,<sup>†,1,2,3</sup> and Baozhong Liu <sup>\*,1,2,3</sup>

<sup>1</sup>CAS and Shandong Province Key Laboratory of Experimental Marine Biology, Institute of Oceanology, Chinese Academy of Sciences, Qingdao, China

<sup>2</sup>Laboratory for Marine Biology and Biotechnology, Pilot National Laboratory for Marine Science and Technology (Qingdao), Qingdao, China

<sup>3</sup>Center for Ocean Mega-Science, Chinese Academy of Sciences, Qingdao, China

<sup>†</sup>These authors contributed equally to this work.

\*Corresponding author: E-mail: bzliu@qdio.ac.cn.

Associate editor: Ilya Ruvinsky

## Abstract

Although a conserved mechanism relying on BMP2/4 and Chordin is suggested for animal dorsal–ventral (DV) patterning, this mechanism has not been reported in spiralian, one of the three major clades of bilaterians. Studies on limited spiralian representatives have suggested markedly diverse DV patterning mechanisms, a considerable number of which no longer deploy BMP signaling. Here, we showed that BMP2/4 and Chordin regulate DV patterning in the mollusk *Lottia goshimai*, which was predicted in spiralian but not previously reported. In the context of the diverse reports in spiralian, it conversely represents a relatively unusual case. We showed that BMP2/4 and Chordin coordinate to mediate signaling from the D-quadrant organizer to induce the DV axis, and Chordin relays the symmetry-breaking information from the organizer. Further investigations on *L. goshimai* embryos with impaired DV patterning suggested roles of BMP signaling in regulating the behavior of the blastopore and the organization of the nervous system. These findings provide insights into the evolution of animal DV patterning and the unique development mode of spiralian driven by the D-quadrant organizer.

**Key words:** dorsal–ventral, mollusk, organizer, BMP, Chordin.

## Introduction

The existence of a dorsal–ventral (DV) axis is a key characteristic in Bilateria. Generally, a conserved molecular logic, namely, the BMP ligand BMP2/4 and its antagonist Chordin, patterns the DV axis of bilaterians (Sasai et al. 1994; François and Bier 1995; Akiyama-Oda and Oda 2006; Lowe et al. 2006; Van der Zee et al. 2006; Lapraz et al. 2009). It has been suggested that these two genes even pattern a body axis in nonbilaterian animal lineages (Saina et al. 2009; DuBuc et al. 2019), indicating broad conservation. However, despite such conservation, the DV patterning mechanism exhibits a considerable degree of variation (Genikhovich et al. 2015). In some cases, DV patterning no longer depends on BMP2/4 and Chordin (e.g., nematodes and ascidians; Patterson and Padgett 2000; Lemaire et al. 2008). In two of the three major bilaterian clades, Ecdysozoa and Deuterostomia, such exceptional cases are considered lineage-specific characters since extensive evidence reveals *bmp2/4-chordin*-dependent mechanisms in their relatives (e.g., insects and vertebrates; Bier and De Robertis 2015; Genikhovich et al. 2015).

The situation in the other bilaterian clade, Spiralia, is very different. Unlike those in ecdysozoans and deuterostomes, the molecular mechanisms of spiralian DV patterning remain largely elusive, and current studies on several representative species have revealed quite diverse results. The role of BMP signaling in DV patterning has not been revealed in the annelid *Chaetopterus pergamentaceus* (Lanza and Seaver 2020a), and it seems to be restricted to the head region in the annelid *Capitella teleta* and the mollusk *Crepidula fornicata* (Lanza and Seaver 2018, 2020b; Lyons et al. 2020; Webster et al. 2021). In the leech annelid *Helobdella robusta*, despite deploying BMP signaling in DV patterning, another BMP antagonist pair (BMP5–8 and Gremlin) is used (Kuo and Weisblat 2011). The roles of BMP2/4 in DV patterning have been shown in two spiralian (the platyhelminth *Dugesia japonica* and the mollusk *Ilyanassa obsoleta*) (Orii and Watanabe 2007; Lambert et al. 2016), yet the roles of Chordin are not investigated. This issue is important since Chordin is suggested to be crucial in DV patterning (Genikhovich et al. 2015), and this gene might have been lost from particular spiralian lineages (e.g., platyhelminths) (Kenny et al. 2014). Otherwise, *chordin*

© The Author(s) 2021. Published by Oxford University Press on behalf of the Society for Molecular Biology and Evolution.

This is an Open Access article distributed under the terms of the Creative Commons Attribution-NonCommercial License (<https://creativecommons.org/licenses/by-nc/4.0/>), which permits non-commercial re-use, distribution, and reproduction in any medium, provided the original work is properly cited. For commercial re-use, please contact [journals.permissions@oup.com](mailto:journals.permissions@oup.com)

Open Access

is indeed retrieved from the genome of spiralian, such as brachiopods (*Terebratalia transversa* and *Novocrania anomala*) and the mollusk *Crassostrea gigas*. In these species, BMP2/4 and Chordin have even been revealed to be expressed oppositely along the DV axis. Nevertheless, although the role of BMP signaling in DV patterning is supported by drug treatment experiments (Martín-Durán et al. 2016; Tan et al. 2017; Tan et al. 2018), the functions of BMP2/4 and Chordin have not been investigated. Altogether, although the ancestral *bmp2/4-chordin*-dependent DV patterning mechanism has been generally accepted for bilaterians (Erwin 2009), studies on nine species spanning four spiralian phyla did not reveal such a mechanism (fig. 1a).

Despite the suggested diversity at the molecular level, spiralian DV patterning actually shows considerable conservation at the cellular level. In spiralian lineages such as annelids, mollusks, and nemerteans, the DV axis is induced by a D-quadrant organizer, referring to a special blastomere that regulates the development of the whole embryo (e.g., 3D or 4d, according to the nomenclature for describing spiral cleavage; see fig. 1b and c) (Henry 2002; Lambert 2010; Seaver 2014). In fact, the involvement of the D-quadrant organizer, in parallel with several other characteristics conserved in this clade but never observed in other clades (e.g., spiral cleavage; but note the suggested modified spiral cleavage in a few nonspiralians (Anderson 1969)), is

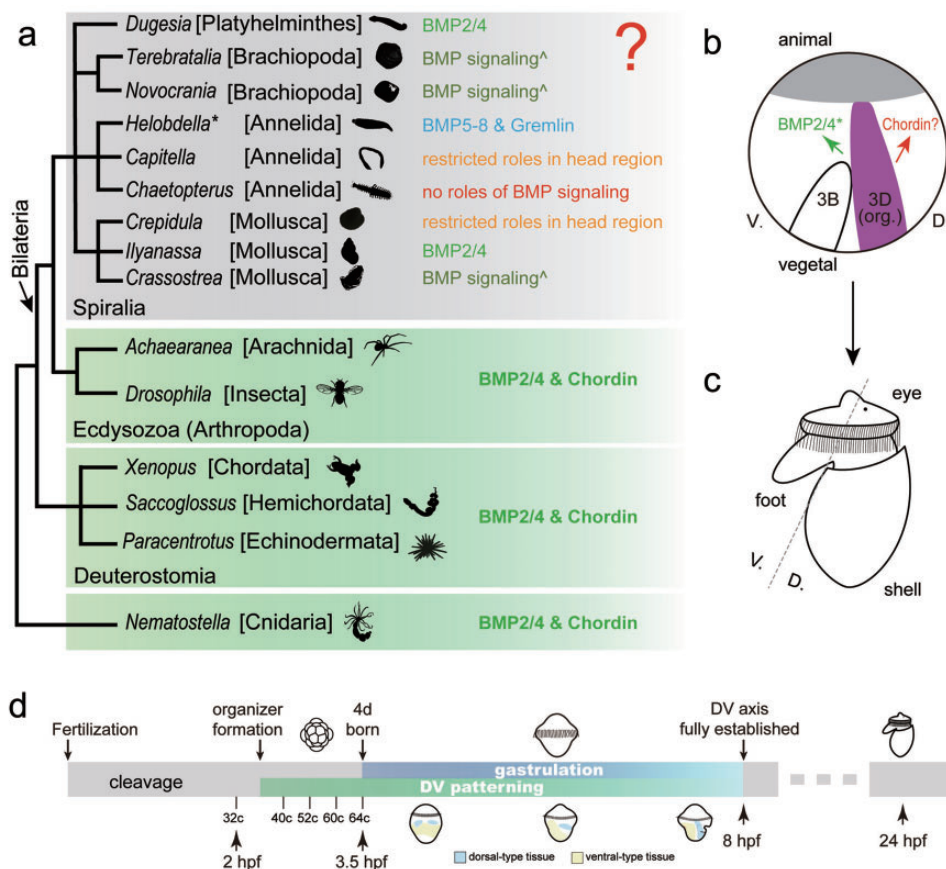


**Fig. 1.** Mollusks represent ideal systems to understand the evolution of animal DV patterning and spiralian organizer function. (a) In most major animal clades, *bmp2/4* and *chordin* determine the secondary body axis (DV axis for bilaterians). For spiralians, however, knowledge is elusive. The carets indicate that in the species, the role of BMP signaling in DV patterning is supported, but the involved molecules remain unknown. Note that here the term “DV patterning” could refer to “DV axis specification” or “patterning along the DV axis” in different organisms. The diagrams of representative animals are derived from PhyloPic (<http://phylopic.org/>, last accessed November 15, 2021) and Wikipedia (<https://www.wikipedia.org>, last accessed November 15, 2021) licensed under CC BY 3.0. (b) A hypothesis regarding the relationships between the organizer and *bmp2/4* and *chordin* in an equal-cleaving mollusk. After formation of the D-quadrant organizer (here referring to the 3D blastomere), it activates BMP signaling by regulating *bmp2/4* (green letters); however, whether *chordin* is involved in this process remains unknown (red letters). The asterisk indicates that this mechanism is reported in an unequal cleaver and it requires validation in equal cleavers. Note that the letters *bmp2/4* and *chordin* in the diagram do not indicate the expression/distribution profiles of the two genes, but simply indicate the presumed regulatory relationships between organizer and the two genes. (c) A veliger larva of gastropod mollusk. The processes regulated by the organizer are highlighted: DV patterning (generally indicated by the dashed line) and the formation of marked larval organs. (d) Early development of the gastropod mollusk *L. goshimai* (at 25°C) emphasizing DV patterning events. Organizer formation is supposed to occur at the 32-cell (32c) stage. This event marks the beginning of DV patterning, which is largely coupled with gastrulation (gastrulation begins at the 64-cell stage once 4d is born.) A DV axis is well established by 8 hpf, and a veliger larva is formed by approximately 24 hpf. The diagrams below the timeline show the development of dorsal- and ventral-type tissues during DV patterning (see details below).

suggested to be the most important developmental characteristic in spiralian (Henry and Martindale 1999; Hejzol 2010; Lambert 2010; Nielsen 2010; Henry 2014). Nevertheless, although the developmental roles of spiralian D-quadrant organizers have been well determined, there is only limited knowledge regarding how they function at the molecular level (Lambert and Nagy 2001; Lambert and Nagy 2003; Koop et al. 2007; Henry and Perry 2008). In this context, investigating the molecular mechanisms of DV patterning would be an essential aspect to decipher the organizer function for spiralian, given the conserved role of organizers in inducing the DV axis.

Interestingly, a link was recently established between the spiralian organizer and the DV patterning gene *bmp2/4*. A pioneering report proved that BMP2/4 mediated organizer signaling and regulated DV patterning in the gastropod mollusk *Ilyanassa* (Lambert et al. 2016), explaining the correlation between organizer function and DV patterning. Despite this essential process, open questions persist. First, it is unknown whether the BMP2/4-dependent organizer function also exists in other spiralian lineages. Investigations of the prevalence of such a mechanism are necessary given the suggested diversity in spiralian DV patterning mechanisms at the molecular level (as mentioned above) and the different dynamics of organizer signaling between species with unequal or equal cleavages (Lambert and Nagy 2001; Lambert and Nagy 2003). Second, and more importantly, whether a BMP antagonist is involved in organizer function should be explored. This question should be clarified since the crucial node in DV patterning is not the BMP ligand itself but the gradient of BMP signaling along the presumed DV axis (Bier and De Robertis 2015). Although the area of intercellular contacts could greatly contribute to the distribution of signaling (Guignard et al. 2020), such a BMP signaling gradient is often regulated by extracellular BMP regulators such as Chordin (Garcia Abreu et al. 2002; Bier and De Robertis 2015). Indeed, restricted *chordin* expression is suggested to be sufficient to determine a BMP signaling gradient, irrespective of the expression patterns of *bmp2/4* (Genikhovich et al. 2015). Thus, despite knowing the involvement of BMP2/4 in organizer function in a representative spiralian, key questions that follow are whether the organizer induces the BMP signaling gradient and, if yes, whether Chordin functions in the process.

Mollusks emerge as ideal systems to clarify the abovementioned questions, that is, whether BMP2/4 and Chordin function in DV patterning of spiralian and the relationship between the two genes and the D-quadrant organizer. The ability of the organizer to induce the DV axis has been well investigated in mollusks (Clement 1962; van den Biggelaar 1977; Guerrier et al. 1978). Although the role of BMP signaling in DV patterning seems to be restricted to the head region in *Crepidula* (Lyons et al. 2020), it has been revealed for the whole larva in *Ilyanassa* (Lambert et al. 2016). As mentioned above, *bmp2/4* and *chordin* are oppositely expressed along the DV axis in *Crassostrea* embryos (Tan et al. 2017), and drug treatment experiments suggest roles for BMP signaling in DV axis formation (Tan et al. 2018). However, gene knockdown

experiments targeting molluscan *bmp2/4* and *chordin* are required to verify this conclusion. Here, we investigated the roles of *bmp2/4* and *chordin* in the equal cleaving mollusk *Lottia goshimai*. Our results suggest that the two genes both regulate DV patterning and participate in organizer function. By examining embryos with impaired DV patterning, we further revealed evidence suggesting the profound developmental effects of stereotype cleavage and the regulatory roles of BMP signaling in the behavior of blastopores and the bilateral organization of the nervous system. These findings provide insights into the unique developmental mode and the evolution of spiralian.

## Results

### The D-Quadrant Organizer and Overall Development of *L. goshimai*

In equal cleaving mollusks (e.g., *Patella vulgata*), one vegetal macromere at the 32-cell stage is induced by micromeres to be the organizer via activation of the MAPK cascade (Lartillot, Lespinet et al. 2002; Lambert and Nagy 2003). However, immunostaining of MAPK signaling indicators (double phosphorylated ERK, ppERK) failed to produce any signals in *L. goshimai* due to technical limits. We therefore sought to identify the organizer of *L. goshimai* based on other evidence. In *Patella*, several characteristics were used to identify the organizer (van den Biggelaar 1977). We found that two of these key characteristics could be observed in *L. goshimai*: prolonged interphase between the 32- to 40-cell stage and a characteristic four-cell arrangement pattern at the vegetal pole of the 60-cell embryo (3D-2d<sup>22</sup>-3c<sup>2</sup>-3d<sup>2</sup>, fig. 2b). These data suggest that, similar to *Patella*, the organizer of *L. goshimai* may also be the 3D blastomere at the 32-cell stage.

When 3D divided to produce 4d, gastrulation began (fig. 1d). Highly similar to *Patella* (Lartillot, Le Gouar et al. 2002; Lartillot, Lespinet et al. 2002; Lyons and Henry 2014), gastrulation in *L. goshimai* was completed through the epiboly of micromeres accompanied by the invagination of macromeres, and DV patterning occurred during this period (fig. 1d). When gastrulation finished at 8 hpf, a DV axis was well established, characterized by a shell field on the dorsal side and a ventral plate and a blastopore on the ventral side (fig. 2c and d). In subsequent development, the larval shell plate (secreted by cells of the shell field) was formed on the dorsal side at 9 hpf; the foot (derived from cells of the ventral plate) emerged on the ventral side at approximately 15 hpf (fig. 2a and e). The larval eyes were recognizable starting at approximately 36 hpf, when a veliger larva was developed (fig. 2a and e).

### Phenotypes after Organizer Inhibition and Manipulating BMP Signaling

If the organizer of *L. goshimai* is indeed the 3D blastomere, inhibiting its formation should cause a deficiency in the development of featured organs. As expected, when we treated the embryo with the MAPK signaling inhibitor U0126 (as described previously; Lambert and Nagy 2001) around the time of organizer formation (from the 16- to the 60-/64-cell

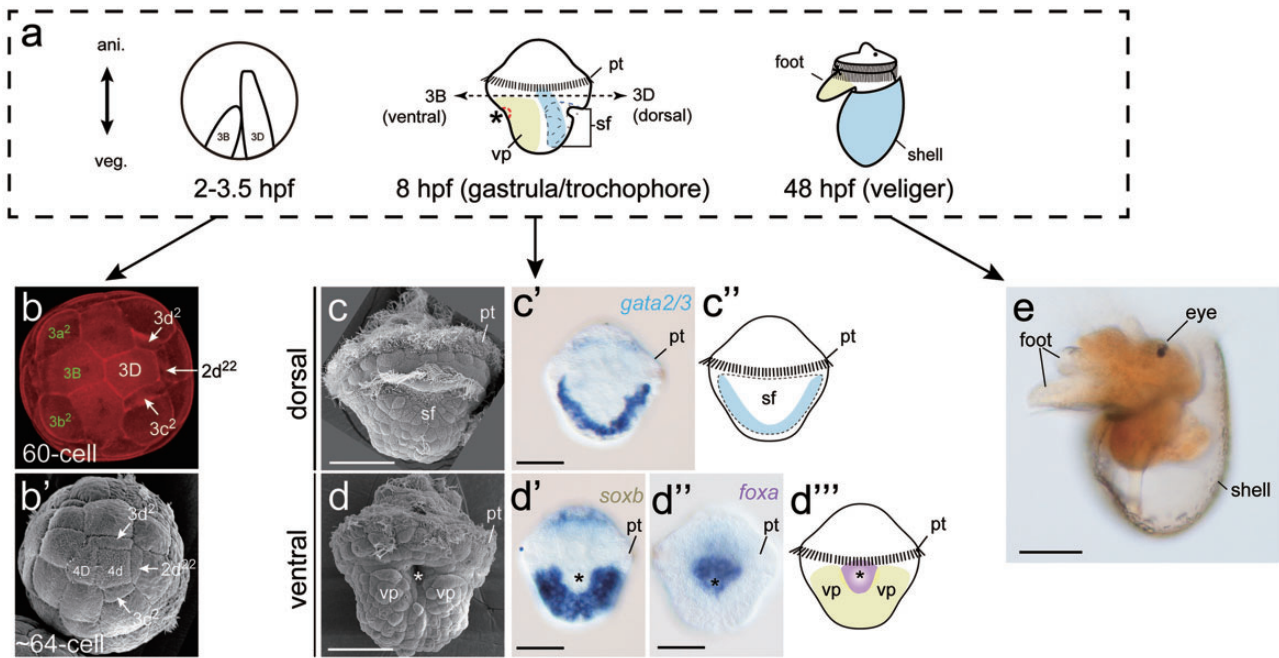


**FIG. 2.** Key aspects of DV patterning in *L. goshimai*. (a) Normal development of *L. goshimai*, lateral views with animal to the top. Key characteristics related to DV patterning are highlighted. Panels (b) and (b') show the vegetal poles of early embryos, in which the characteristic four-cell arrangement patterns are labeled, that is, a more centered macromere (3D) surrounded by three small blastomeres, 2d<sup>22</sup>, 3c<sup>2</sup>, and 3d<sup>2</sup> (in b', 3D has divided to produce 4D and 4d). Panels (c) and (d) show the embryo with a well-established DV axis: shell field (sf) on the dorsal side and ventral plate (vp) and blastopore (the asterisk) on the ventral side, which could be marked by expression of the marker genes *gata2/3* (c'), *soxb* (d'), and *foxa* (d''), respectively. Panel (e) shows a veliger larva in which the organs induced by the organizer (shell, foot, and eye) are indicated. pt, prototroch. The bars represent 50 μm.

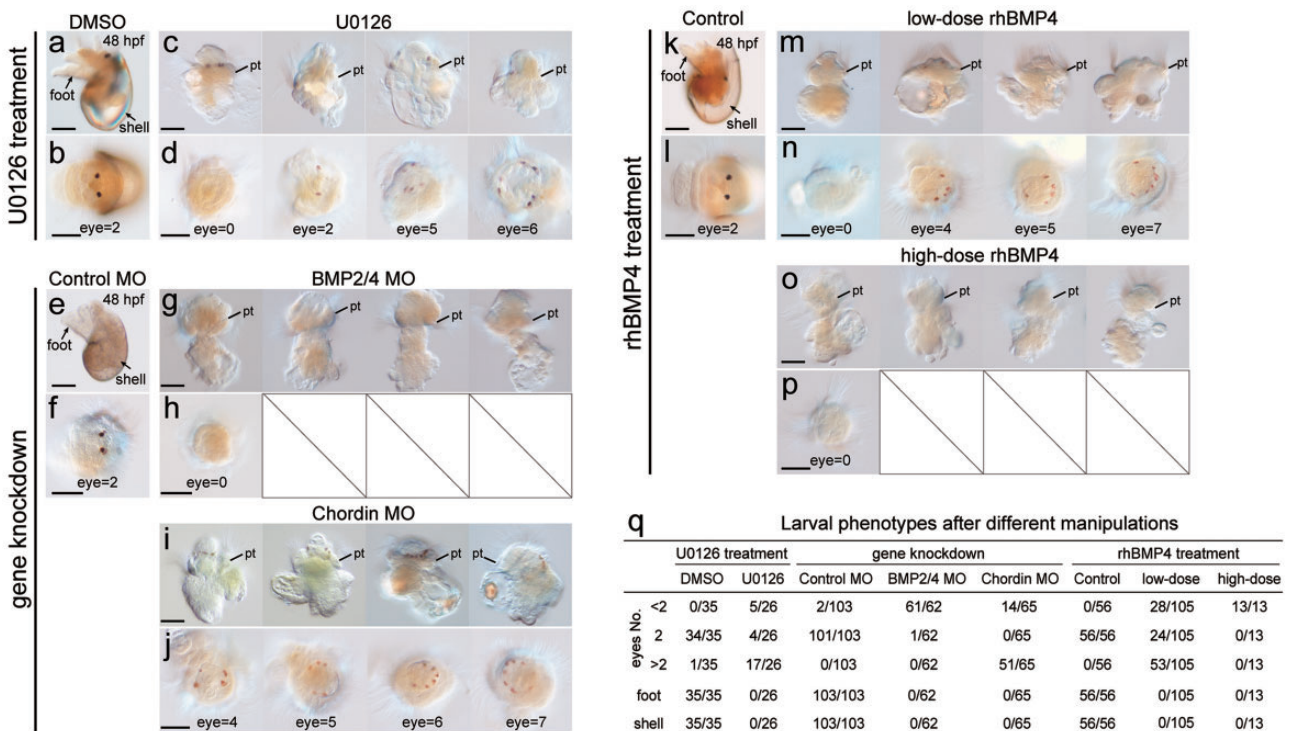


**FIG. 3.** Larval phenotypes after different manipulations. Panels (a–p) show the manipulated larvae. In each group, the general larval morphology is shown in the upper panels (lateral views with anterior to the top), and larval eyes are shown in the lower panels (anterior views); note that there are no one-to-one relationships between the upper and lower panels of each group. Multiple individuals are shown since the larval morphology showed heterogeneities to varied extents. Panel (q) shows a statistical summary, and the details of eye development are shown in [supplementary figure S2a, Supplementary Material online](#). pt, prototroch. The bars represent 50 μm.

stage), the shell and foot largely failed to form, and larvae possessed extra eyes (fig. 3*a–d* and *q*). This phenotype is highly similar to that in the equal-cleaving mollusk *Tectura* (Lambert and Nagy 2003). The finding that short-term treatment with U0126 caused serious developmental deficiency is consistent with the notion that the time window of organizer signaling is quite narrow (although we did not precisely determine it).

We then explored the developmental roles of *bmp2/4* and *chordin* by injecting oocytes with specific morpholinos (MOs); treatment experiments using a recombinant human BMP4 protein (rhBMP4) were also performed for comparison. Knockdown of *bmp2/4* or *chordin*, as well as rhBMP4 treatment, produced larval phenotypes with no shell or foot (fig. 3*e–q*). Eye development differed among different manipulations: no eyes developed after *bmp2/4* knockdown (fig. 3*h*) and high-dose (0.5  $\mu\text{g}/\text{mL}$ ) rhBMP4 treatment (fig. 3*p*), and extra eyes were observed after *chordin* knockdown (fig. 3*j*) and a low-dose (0.075  $\mu\text{g}/\text{mL}$ ) rhBMP4 treatment (fig. 3*n*). Taken together, despite the varied specific effects on eye development, manipulation of BMP signaling, either by gene knockdown or rhBMP4 protein treatment, caused abnormal development of organizer-induced organs, comparable to the phenotype after U0126 treatment.

However, it was difficult to directly interpret these larval phenotypes. We therefore analyzed multiple developmental stages to dissect how development was altered under these manipulations and focused on the roles of *bmp2/4* and *chordin*. In particular, very early embryos ( $\sim$ 60-cell stage) were used to explore whether the two genes mediated organizer signaling; embryos during gastrulation (6 and 8 hpf) were used to explore their roles in DV patterning; and veliger larvae (15 and 48 hpf) were used to investigate the effects of BMP signaling on the nervous system. Given that the samples we analyzed spanned from very early embryos with a single animal–vegetal (AV) axis to late larvae possessing all three body axes, we used the following terms to avoid confusion regarding body orientations. For the embryos before gastrulation was finished (embryos at 8 hpf and earlier stages), the primary body axis was consistently referred to as the AV axis (although it could be called the animal–posterior [AP] axis in the 8-hpf embryo), and the DV axis (when discriminable) was described as the axis perpendicular to the AV axis. For the larvae after gastrulation (herein referring to the larvae at 15 hpf and later stages), their AP and DV axes were described as conventionally used.

### *bmp2/4* and *chordin* Mediate Organizer Signaling and Determine the BMP Signaling Gradient in the Early Embryo

We first focused on the period around the time of organizer formation, that is, from the 16- to the 64-cell stage. The expression of *bmp2/4* and *chordin*, as well as the dynamics of BMP signaling (reflected by the key signal transducer phosphorylated Smad1/5/8 [pSmad1/5/8]), was explored during this period. Radial expression of *bmp2/4* was stably detected in 1q descendants with minor changes (see details in fig. 4*a–*

*d*). In contrast, we found a strong correlation among *chordin* mRNA expression, pSmad1/5/8 activity, and the organizer (fig. 4*e–l*). In brief, sequential developmental events were noticed: (1) suspected organizer formation at the 32-cell stage, (2) activation of uniform pSmad1/5/8 activity since the late 32-cell stage (fig. 4*j*), (3) transition of *chordin* expression into an asymmetrical pattern since the 32- to 40-cell stage (fig. 4*g*), and (4) transition of pSmad1/5/8 activity into an asymmetrical pattern since the 52-cell stage (fig. 4*l*). In the 60-cell embryo, the cells adjacent to the organizer showed strong pSmad1/5/8 activities, while only weak activities were detected in the cells distal to the organizer (fig. 4*l*). This distribution pattern is comparable to the BMP signaling gradient along the DV axis in many animals (e.g., *Drosophila* and sea urchin; Wang and Ferguson 2005; Lapraz et al. 2009); we thus refer to it as the BMP signaling gradient, although it does not exhibit an exact gradient pattern. Since the direction of this gradient was across the 3D and 3B blastomeres that generally coincided with the presumptive DV axis (Henry and Martindale 1999; Lambert 2010), this BMP signaling gradient marked a molecular DV axis prior to the morphologically detectable DV axis.

The correlations among the organizer, *chordin* expression and BMP signaling suggest regulatory relationships. We first confirmed that organizer formation likely triggered BMP signaling. When organizer formation was inhibited by U0126 treatment (fig. 5*Ab*), pSmad1/5/8 activity was diminished (fig. 5*Ai*). On the other hand, since the activation of pSmad1/5/8 activity at the 32-cell stage was uniform, we could not deny the possibility that such activation is independent of the organizer function but simply related to cell cycle. In this context, the decreased pSmad1/5/8 activity after U0126 treatment could be explained by the sustained *chordin* expression in the 3D blastomere of the manipulated embryos (fig. 5*B*; see details later). We next found that the activation of pSmad1/5/8 activity at the 32-cell stage was mostly mediated by *bmp2/4* because injecting an antisense BMP2/4 MO greatly reduced pSmad1/5/8 staining (fig. 5*Ak*), while 3D was born at the normal time and with similar morphology (fig. 5*Ad*). Consistent to this notion, ectopic rhBMP4 treatments caused an upregulation of pSmad1/5/8 on the 3B-side blastomeres of the embryos (fig. 5*An*). However, the activity of pSmad1/5/8 upon initial activation showed only a uniform distribution. We revealed that Chordin was required to create the graded pattern of pSmad1/5/8. When *chordin* was inhibited by injecting an antisense MO, no gradient was formed, and uniform pSmad1/5/8 activity was sustained (until at least the 64-cell stage, fig. 5*Al*), despite the morphologically normal organizer (fig. 5*Ae*). We further found that *chordin* expression was regulated by the organizer. After U0126 treatment, asymmetric *chordin* expression no longer emerged: its uniform expression in all 3Q blastomeres was sustained, and its (asymmetrical) expression in micromeres was not activated (fig. 5*Bg–Bl*).

Based on these results, we concluded that regulatory relationships existed between the organizer and *bmp2/4* and *chordin* in *L. goshimai* (fig. 5*C*). In brief, after the formation of organizer induced by micromeres (fig. 5*Ca–Cb*), the

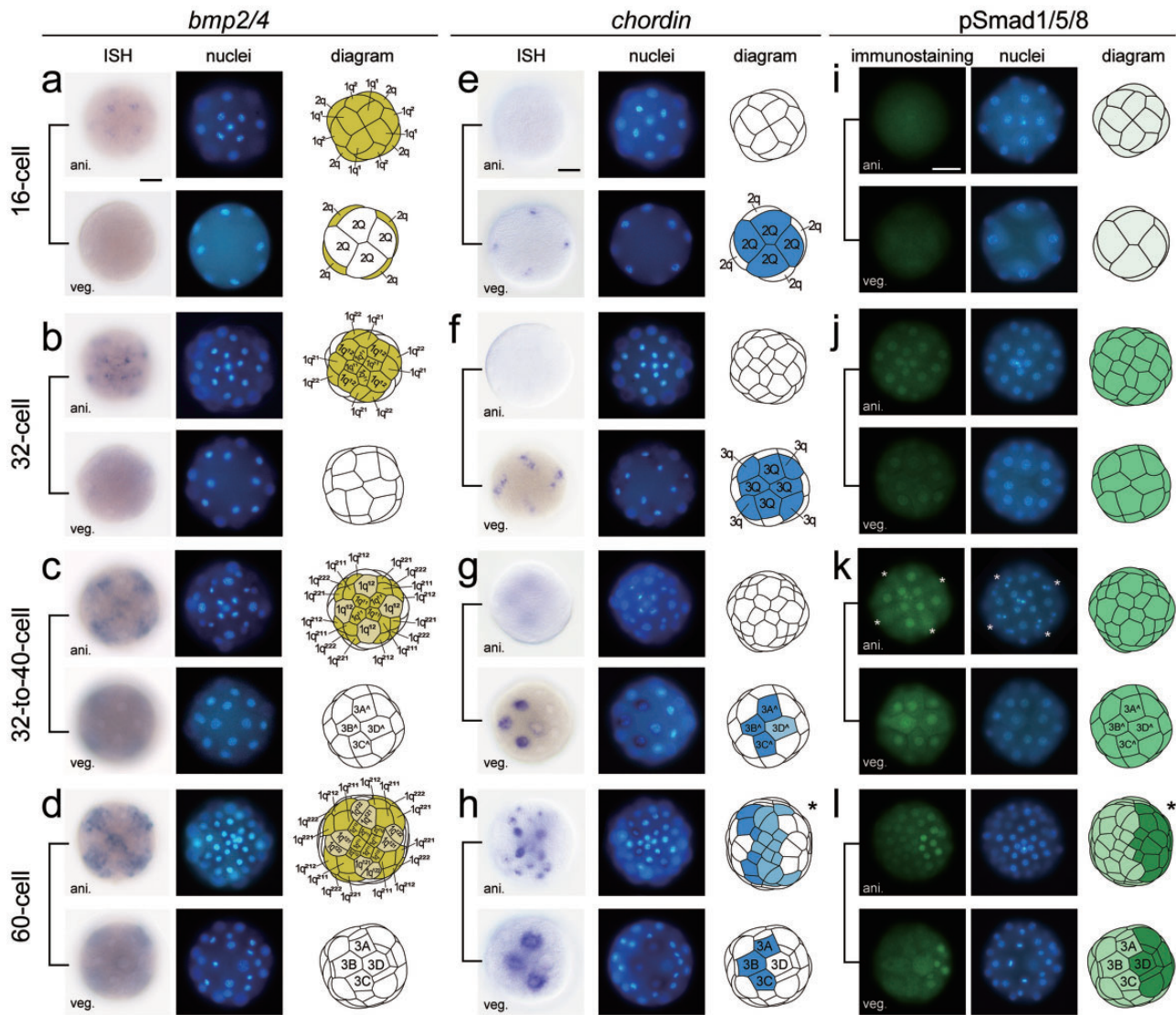


**Fig. 4.** Normal *bmp2/4* and *chordin* mRNA expression and pSmad1/5/8 activities during the periods before and after organizer formation. In each panel, the animal (ani.) and vegetal (veg.) views of the stained embryo are shown along with corresponding diagrams. The blastomeres showing gene expression are indicated in the diagrams, and those at the 60-cell stage are shown in [supplementary figure S1a–d, Supplementary Material online](#) (black asterisks in *h* and *l*). Note that although it could not be clearly discriminated in the figures, we confirmed *bmp2/4* mRNA expression in 2q at the 16-cell stage (*a*) and in 1q<sup>12</sup> and its descendants at later stages (*b–d*); also, very weak but detectable pSmad1/5/8 activity could be observed in 16-cell embryos (*i*). In (*k*), the absence of pSmad1/5/8 staining in 1q<sup>2</sup> descendants (white asterisks) was caused by the active dividing of the cells, and we found that the signals were restored after cell division was completed. The carets in (*c*), (*g*), and (*k*) indicate that the 3Q macromeres were actually not distinguishable from each other based on morphology, despite 3D showing decreased *chordin* expression (*g*).

organizer seems to trigger BMP2/4 (green arrows in [fig. 5Cb](#)), which induces uniform BMP signaling activities ([fig. 5Cc](#)). Alternatively, the activation of BMP2/4 at the 32-cell stage may be related to cell cycle and independent of organizer function. Shortly afterward, the organizer regulates *chordin* expression to form an asymmetrical pattern, including both the downregulation in the 3D blastomere and the upregulation in the 3B-side micromeres. The asymmetrical expressed *chordin* modulates BMP signaling to form a gradient along the presumptive DV axis ([fig. 5Cd](#)). These sequential events explain the time lag between the (suspected) time point of organizer formation at the 32-cell stage and that of the emergence of the BMP signaling gradient after the 52-cell stage.

### Roles of *bmp2/4* and *chordin* in DV Patterning Normal DV Patterning and *bmp2/4* and *chordin* Expression in the Ectoderm during Gastrulation

We next focused on the DV patterning process. The DV patterning of *L. goshimai* was largely coupled with gastrulation. We firstly explored the process using SEM. Although most ectodermal cells were morphologically similar in the embryos, the endodermal cells and the ectodermal cells surrounding them could be recognized by the long and short protrusions on their surface, respectively (highlighted in [fig. 6Af](#)). We found that with gastrulation proceeded, the blastopore moved from posterior to ventral; and the tissues adjacent to blastopore showed a similar trajectory,

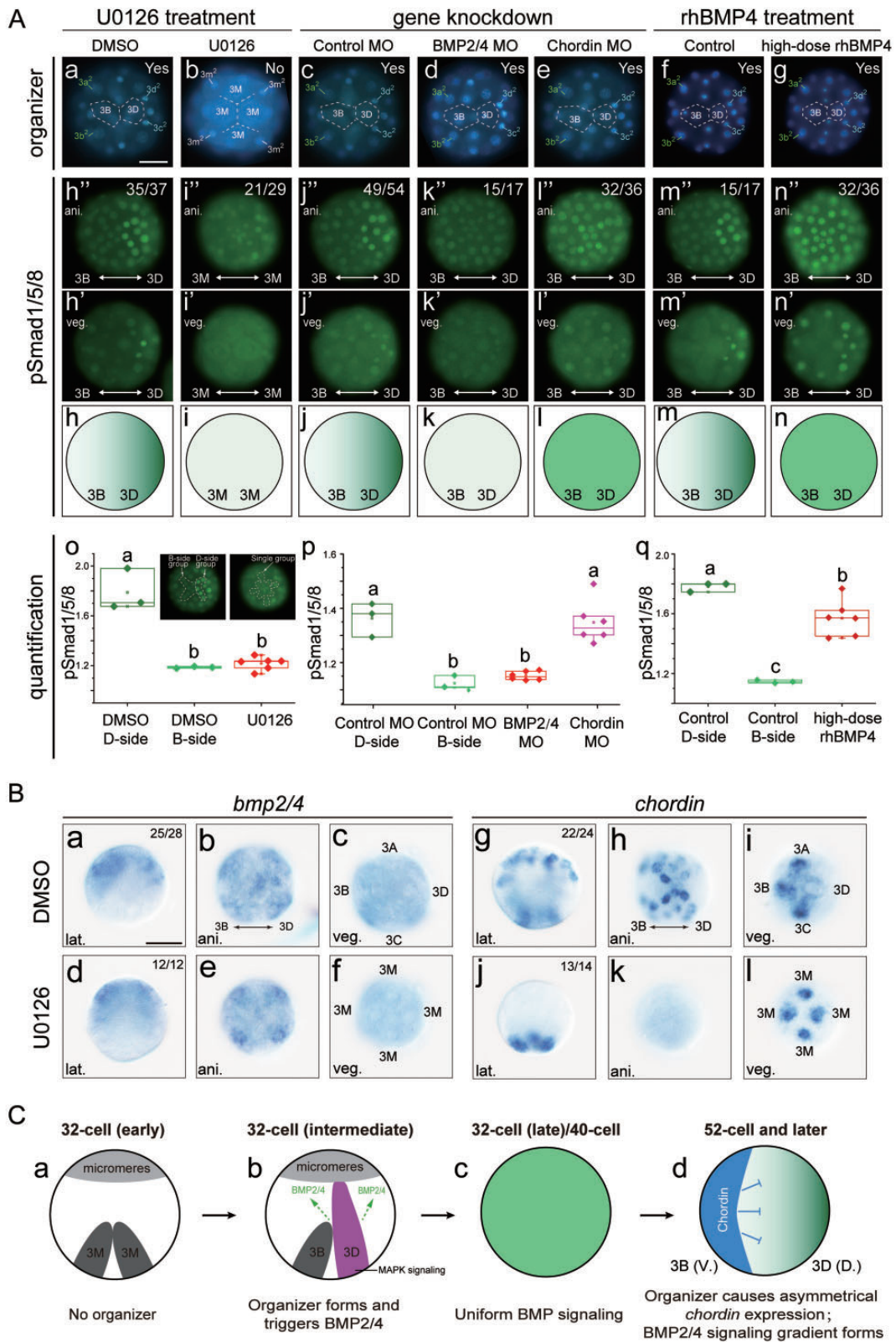


**FIG. 5.** Regulatory relationships among the organizer, *bmp2/4* and *chordin*. (A) The states of organizer and pSmad1/5/8 activities under different manipulations; all samples at the 60- or 63-cell stage. In (Aa)–(Ag), the organizer is identified based on the cell arrangement pattern at the vegetal pole (see Fig. 2b); and whether an organizer was formed is indicated by “yes” or “no” in the panels. Panels (Ah)–(An) show diagrams of pSmad1/5/8 staining along the 3B–3D axis (lateral views with the animal pole to the top); animal and vegetal views are shown in the upper rows. pSmad1/5/8 activities were estimated by quantifying the signaling in 12 blastomeres at the animal pole, and the results are shown in (Ao)–(Aq). The inserts in (Ao) show how the 12 blastomeres were grouped (also applied to Ap and Aq): they were divided into D- and B-side groups for control embryos and considered as a single group for manipulated embryos. Note that during quantification, the fluorescence intensity was recorded for each nucleus

indicating morphogenetic changes along the DV axis (fig. 6A).

We then investigated marker gene expression to explore more information. The marker genes included *gata2/3*, which was expressed on the outer edge of the shell field (fig. 2c'); *soxb*, which was expressed on the ventral plate (fig. 2d'); and *foxa*, which marked the blastoporal tissues (fig. 2d''). We largely focused on gene expression in the ectoderm, given it provided the most essential information of the morphogenetic changes during gastrulation. The results revealed that at the initial phase of DV patterning (4.3–5 hpf), the anlagen of the shell field and ventral plate were generally aligned along the AV axis (fig. 6Ba–Bb and Be–Bf) and organized in almost circular patterns along the presumptive DV (3B–3D) axis (fig. 6Ba'–Bb' and Be'–Bf'). During subsequent development, despite minor changes, the gene expression regions remained circular organizations; but their locations continuously changed, and finally became restricted to dorsal and ventral sides (fig. 6Ba–Bp). The high consistent trajectory between the *soxb*-expressing region and that of the tissues adjacent to the blastopore (compare fig. 6A and Be–Bh) indicates that the changes in the gene expression regions should largely attribute to morphological changes during gastrulation. Altogether, SEM and gene expression data revealed that during gastrulation, the blastopore (and related tissues) moved from posterior to ventral, and many gene expression patterns that were generally broad and mostly radial became restricted along the DV axis (red dashed arrows in fig. 6Ba–Bh).

We explored the expression of *bmp2/4* and *chordin* during this period. Retrochordal expression of the two genes was generally distributed in a few dorsal/ventral cells, despite minor changes in the numbers and locations of the cells (supplementary fig. S3e–l, Supplementary Material online). In the posttrochial region, *bmp2/4* expression was first detected in two groups of lateral cells at 5 hpf (fig. 6Br and Br'), then formed a semicircular expression pattern at 6 hpf (fig. 6Bs and Bs'), and finally transitioned to a U-shaped pattern restricted to the shell field edge (fig. 6Bt and Bt'). In general, it experienced dynamics similar to those of *gata2/3* expression (compare fig. 6Bq–Bt and Ba–Bd). Similarly, the dynamics of *chordin* expression were comparable to those of *soxb* and *foxa* expression. We first detected two expression regions on the dorsal and ventral sides at 5 hpf (fig. 6Bv and Bv'). At 6 hpf, the expression on the ventral side was detected in two bilateral groups of cells, seemingly related to blastoporal tissues (arrowheads in fig. 6Bw and Bw'), and the expression in the dorsal region had expanded and “moved” to the vegetal pole

(triangles in fig. 6Bw and Bw'). At 8 hpf, *chordin* expression was mostly detected in the ventral plate (fig. 6Bx and Bx'), although it seemed to cover fewer areas than *soxb* (compare fig. 6Bx' and Bh').

#### Radialized Early Development: *bmp2/4* and *chordin*-Dependent DV Patterning

We analyzed the changes in DV patterning under different manipulations based on marker gene expression. Inhibition of molluscan organizers results in loss of the DV axis and radialized development (Martindale et al. 1985; Kührtreiber et al. 1988). Consistent with this finding, after U0126 treatment, the expression of three marker genes all showed radial patterns in 6-hpf embryos (fig. 7g, i, and j), in contrast to the evident asymmetrical gene expression in normal embryos (fig. 7a–e). The *bmp2/4* and *chordin* expression was seriously inhibited after U0126 treatment (fig. 7f and h), and *bmp2/4* expression did not show a consistent pattern (supplementary fig. S3m–q, Supplementary Material online). After *bmp2/4* or *chordin* knockdown in embryos, as well as after high-dose rhBMP4 treatment (the low-dose rhBMP4 treatment seemed to not efficiently inhibit DV patterning and thus is not discussed hereafter, see supplementary fig. S2b–n, Supplementary Material online), the marker genes and *bmp2/4* and *chordin* all showed radial expression (fig. 7k–y; despite significant differences in the morphologies of the embryos), although *foxa* expression showed a trend of asymmetry (fig. 7o and t). We also confirmed that another two marker genes (*hox1* and *hsp90a*) exhibited similar radial expression after these manipulations (supplementary fig. S4, Supplementary Material online). Altogether, these data supported radialized development after inhibiting organizer function or manipulating BMP signaling.

The highly similar radialized development caused by either inhibiting organizer formation or manipulating BMP signaling indicated that they indeed reflected the deficiency in DV patterning. The common characteristic of the radialized embryos was that the dorsal/ventral marker expression was not greatly disrupted (despite limited exceptions, e.g., the loss of posttrochial *bmp2/4* expression after *chordin* knockdown; fig. 7p), but instead of showing restricted dorsal/ventral localizations, they were radially organized (fig. 7). Although for each gene, the radial expression could be interpreted to represent the activation of gene expression on the opposite side to the normal expression region, this is unlikely the case. In fact, the radial expression patterns after manipulations

but not for an area (see more information in supplementary text, Supplementary Material online and supplementary fig. S1, Supplementary Material online). (B) Changes in *bmp2/4* and *chordin* mRNA expression after U0126 treatment. (C) A hypothesis assuming regulatory relationships among organizer, *bmp2/4*, and *chordin*. When the 32-cell embryo initially forms, the four macromeres (3M) are equivalent (Ca). One of them is subsequently induced to be the organizer (3D) due to the establishment of direct contact with micromeres at the animal pole; MAPK signaling is then activated in this blastomere (Cb). The organizer seems to trigger BMP2/4 (Cb), which induces uniform BMP signaling activities (Cc). The green dashed arrows in (Cb) indicate that it is possible that the activation of BMP2/4 (and the BMP signaling) may be related to cell cycle and is independent of the organizer. Subsequently, the organizer regulates *chordin* expression to form an asymmetrical distribution, which further transforms BMP signaling into a gradient pattern (Cd). See more information in the text. Note that we speculated regulatory roles of organizer on Chordin (and possibly BMP2/4) in widespread blastomeres that are not restricted to 3D itself; this may be explained by the extensive contact of 3D with other blastomeres or the employment of paracrine signaling.



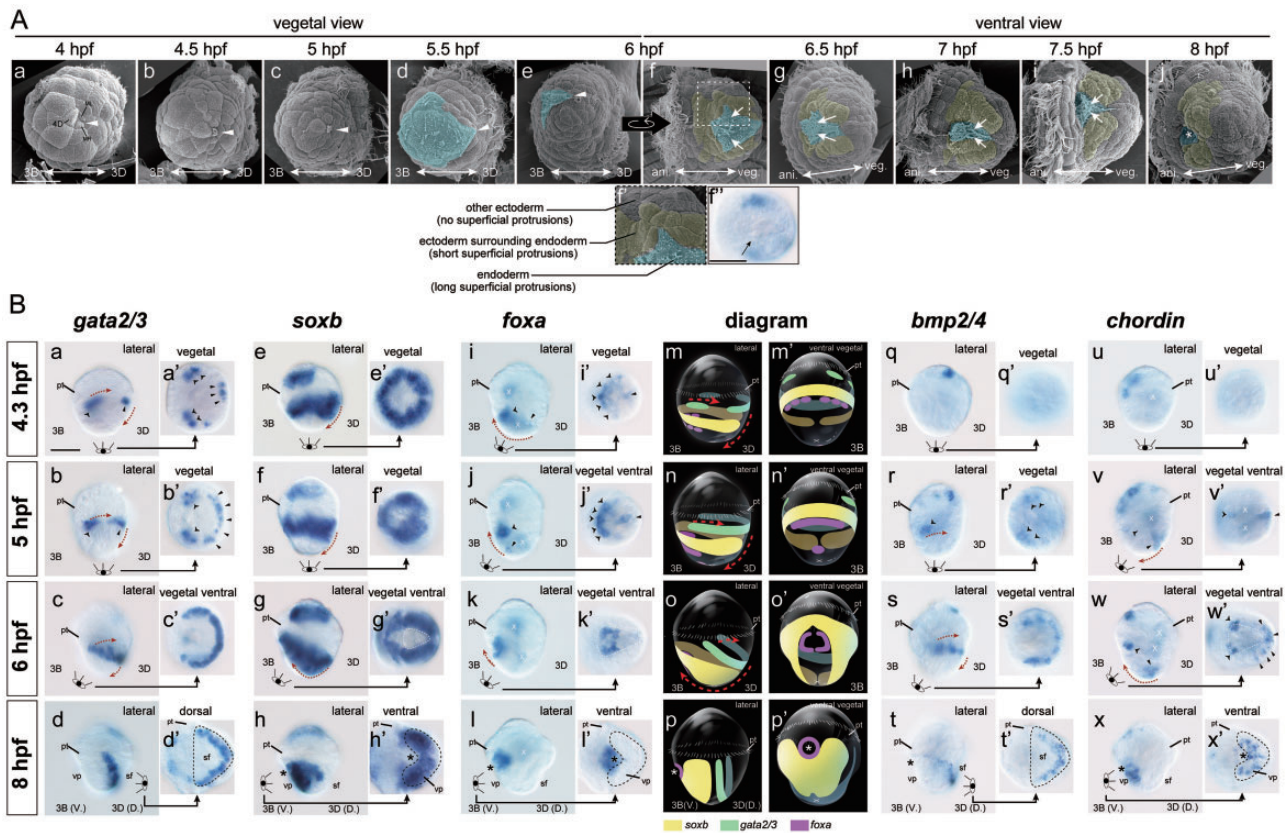


**FIG. 6.** Normal DV patterning of *L. goshimai* and *bmp2/4* and *chordin* expression in the ectoderm during gastrulation (4–8 hpf). Panel (A) shows SEM images during gastrulation. Panel (A $f'$ ) shows a magnified image of the region enclosed by the dashed rectangle in (A $f$ ). At 4 hpf, the descendants of 3D (4D and the 4d-derived ML and MR) first invaginated, causing the formation of a small depression that could be used as a landmark for subsequent analysis (white arrowheads in Aa–Ae). This depression was generally located on the dorsal part of the vegetal pole until 5.5 hpf, when the endodermal tissues developed long superficial protrusions (highlighted by the blue shadowed area in Ad–Aj, see details in A $f'$ ). At 6 hpf, the surface of the exposed endoderm greatly decreased (compare Ad and Ae), likely reflecting quick internalization of the endoderm. From vegetal ventral view, the uninternalized endodermal tissues showed a triangular shape (A $f'$ ) and could be roughly recognized under an ordinary microscope (the arrow in A $f'$ ; this region is indicated by white dashed lines in Bg', Bk', and Bw'). At this stage, the ectodermal cells encompassing the uninternalized endodermal tissues exhibited short protrusions on their surface (highlighted by the yellow shadowed area in A $f'$ –Aj, see details in A $f'$ ). During subsequent development, the endodermal tissues continued to become internalized, and the ectodermal cells encompassing them gradually “moved” toward animal pole as well as the midline (white arrows in A $f'$ –Ai). Together, the morphogenetic changes during gastrulation caused the blastopore (tissues surrounding the endoderm) to move from vegetal pole to ventral side (compare Ad and Aj). Panel (B) shows the expression of marker genes as well as that of *bmp2/4* and *chordin* during gastrulation. Three marker genes were used: *gata2/3* (in shell field), *soxb* (in ventral plate), and *foxa* (in blastoporal rim) (see fig. 2). For each gene, the left panels show lateral views with the animal pole to the top (Ba–Bl), and the right, smaller panels show the view from which the clearest gene expression pattern could be observed (e.g., vegetal or ventral vegetal views, Ba'–Bl'). When the expression is somewhat scattered, corresponding expression regions are indicated by arrowheads and triangles (e.g., in Ba and Ba'). The white crosses indicate signals in endo/mesodermal tissues; they were ignored given that the most important information could be obtained from ectodermal tissues. Generally, our results suggest the expression regions of these genes showed continuous changes (red dashed arrows in Ba–Bp). Panels Bq–Bx show *bmp2/4* and *chordin* expression during this stage. The asterisks indicate the blastopore. pt, prototroch; sf, shell field; vp, ventral plate. The bars represent 50  $\mu$ m.

seemed to represent an “arrest” state, since they were actually comparable to the gene expression patterns in normal embryos at the earlier stage of DV patterning (e.g., at 4.3 or 5 hpf; for extreme examples, compare fig. 6Bb' and 7l' and fig. 6Be' and 7n'/s'). Our results indicate that during normal development, early circular gene expression became restricted to dorsal/ventral regions through complicated morphogenetic changes (fig. 6). Therefore, it seems that the morphogenetic changes were altered after the manipulations (however, one should not simply propose a direct regulatory relationship).

In addition, our results suggested the roles of BMP signaling in regulating cell specification. Although we emphasized

marker gene expression in the posttrochal region in the above descriptions, it is notable that pretrochal gene expression was also radialized after manipulations (when detectable; referring to *bmp2/4*, *chordin*, and *soxb*, fig. 7). Moreover, based on SEM (not shown) and gene expression data (supplementary fig. S3a–d, Supplementary Material online), we did not notice extensive morphogenetic changes in the pretrochal region comparable to those in the posttrochal region. Therefore, radialized gene expression in the pretrochal region might be caused by changes in cell specifications.

Altogether, our results indicate different aspects of the roles of BMP signaling: 1) it is involved in the morphogenetic

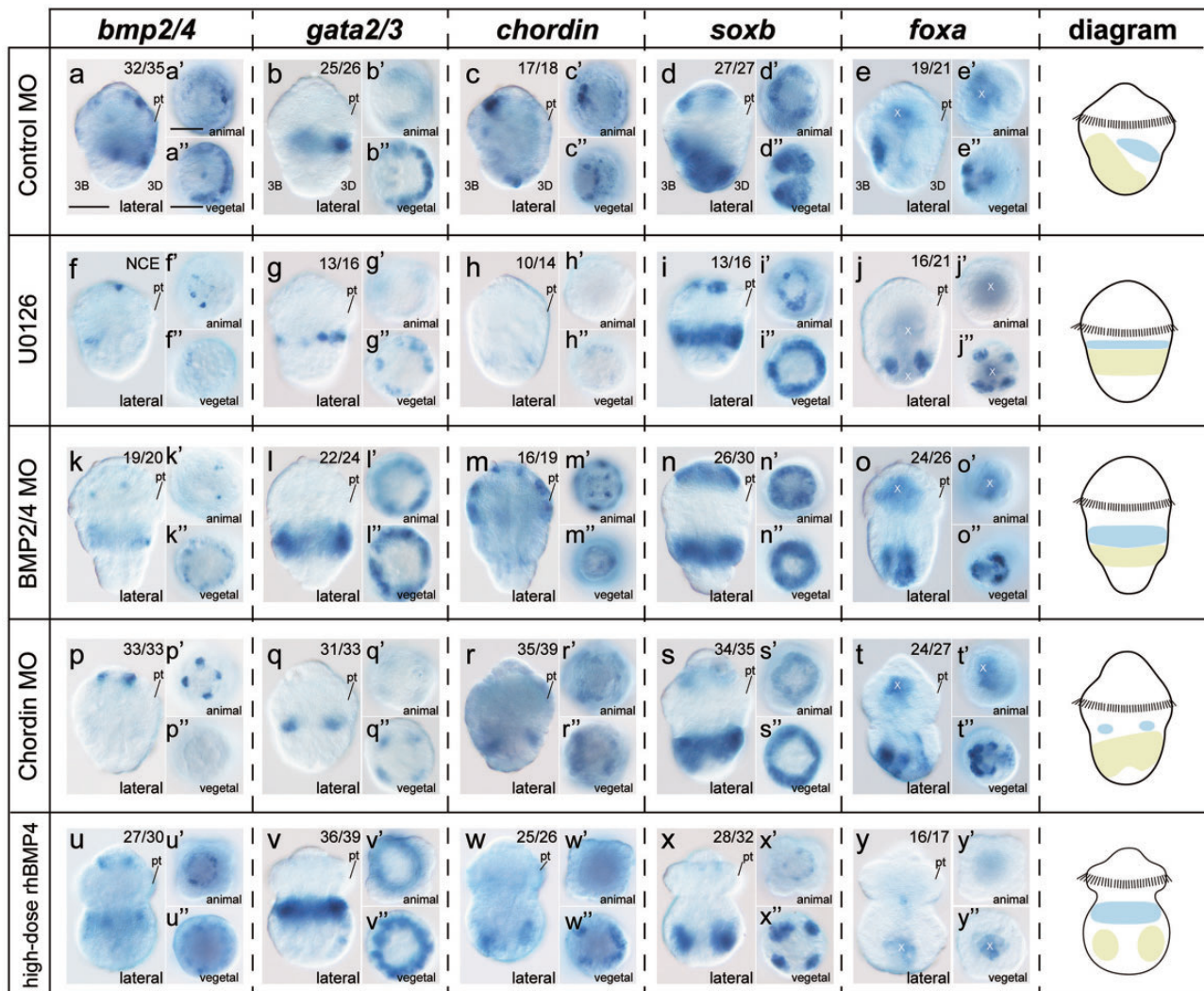


**Fig. 7.** Radialized development at 6 hpf after organizer inhibition or manipulations of BMP signaling. Lateral views (animal to the top) are provided in the left panel, and animal and vegetal views are shown in the right panels. Gene expression patterns were similar in embryos of different control groups (treated with DMSO, a blank solution of rhBMP4, or injected with control MO); thus, only those injected with control MO are shown here. Evident asymmetrical expression along the DV axis could be observed for each gene in control embryos (note that the expression of a dorsal/ventral marker gene still spreads to the opposite side due to the unfinished gastrulation at this stage). After manipulations, the marker genes, as well as *bmp2/4* and *chordin* themselves, generally show radial expression, despite the polarities observed for *foxa* expression. The diagrams are derived from the expression patterns of *gata2/3* (dorsal-type tissues) and *soxb* (ventral-type tissues). Note that there was no consistent expression pattern for *bmp2/4* after U0126 treatment (indicated by NCE in *f*). The lack of poststrochal *bmp2/4* expression after *chordin* knockdown (*p* and *p''*) indicates an inhibitory effect of BMP signaling on *bmp2/4* expression in this region. Minor polarity was observed for the expression of *chordin* (*r*) and *soxb* (*s*) in *chordin*-knockdown embryos. The white crosses indicate endo/mesodermal staining, which was not discussed in most cases, but its location at the center of the vegetal pole in rhBMP4-treated embryos provides evidence supporting radialized development (*y* and *y''*; ectodermal *foxa* expression was not detectable in these embryos). pt, prototroch. The bars represent 50  $\mu$ m.

changes in the poststrochal region that contribute to DV patterning and 2) in the pretrochal region, it seems to participate in cell specifications along the DV axis. It should be noted that in any case, our results indicate correlations between BMP signaling and the related cellular processes but are not indicating direct regulatory effects.

#### Reemerged Asymmetrical Development and Posteriorized Blastopores in Late Embryos

The gene knockdown embryos actually exhibited minor asymmetry at 6 hpf (fig. 7*r* and *s*), and we found that this

asymmetry could be significantly amplified in subsequent development. When gastrulation was completed at 8 hpf, the expression of marker genes reflected the well-developed DV axis in normal embryos (fig. 8*b–f*). Due to the impaired DV patterning, the *bmp2/4*-knockdown embryos largely retained radialized development (fig. 8*h–l*). Only minor asymmetry was detected (e.g., polarized *chordin* expression; fig. 8*j* and *j'*); we could not determine the direction of the asymmetry. In contrast, asymmetrical development in the *chordin*-knockdown embryos was much more evident (fig. 8*n–r*). Such asymmetry occurred along the 3B–3D axis (see supplementary fig. S5*a–h*, Supplementary Material online for details on

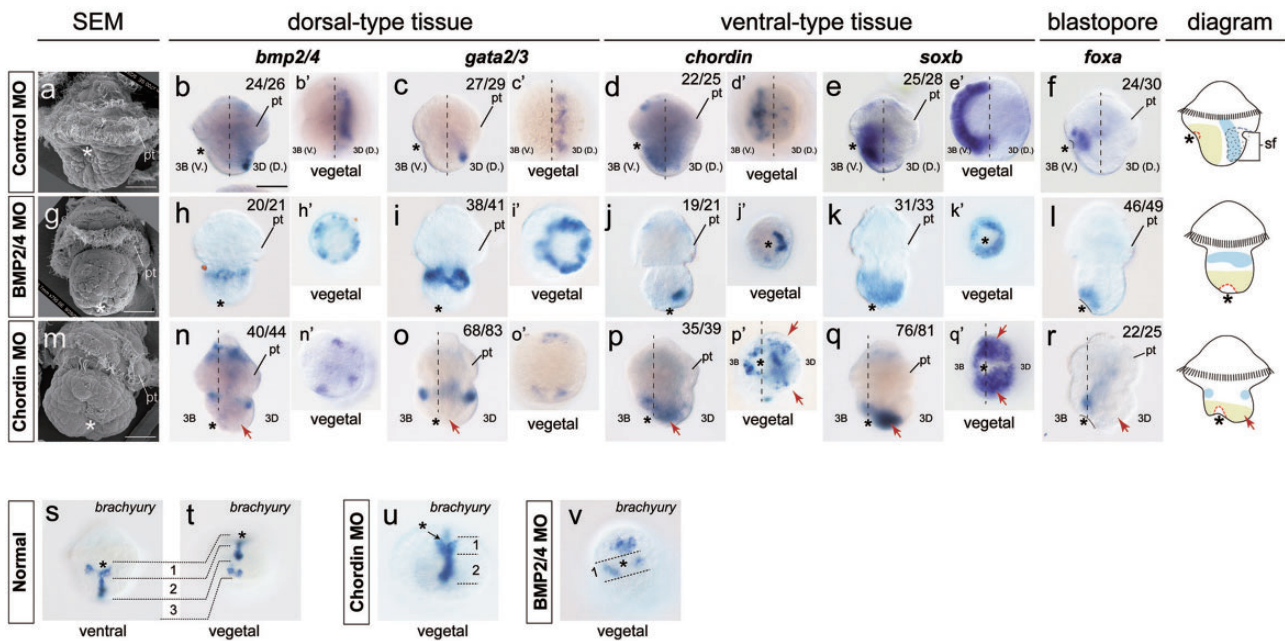


**Fig. 8.** *bmp2/4* and *chordin* knockdown phenotypes at 8 hpf. Except for the SEM images, panels (a)–(r) show lateral views with the 3B side to the left (when discriminable, indicated by dashed lines). The diagrams show the body plans derived from the marker gene expression patterns shown in other panels. Radialized development was largely sustained in the *bmp2/4*-knockdown embryos (g–l), despite polarized expression of *chordin* (j). However, evident asymmetry was observed for *chordin*-knockdown embryos (red arrows in n–r); referring to the much-expanded *soxb*-expressing tissues on the 3D side comparing to those on the 3B side (q and q', note the dashed lines separating the 3B and 3D sides). Expression of the blastopore marker *foxa* indicates that the locations of the blastopore (asterisks) are very different in control embryos (f) and manipulated embryos (l and r). Panels (s)–(v) show *brachyury* expression at 8 hpf. At this stage, normal *brachyury* expression comprises three parts (indicated by numbers in s and t; see the text for more information). After gene knockdown, expression part 1 could be discriminated in both types of embryos (u and v), while expression part 2 was only observed in the *chordin*-knockdown embryo (u). pt, prototroch. The bars represent 50  $\mu$ m.

the orientation of the manipulated embryos). In particular, in the posterior part of the embryo, the 3D side exhibited much greater development than the 3B side (red arrows in fig. 8n–r), which showed *soxb* expression marking ventral-type tissues (fig. 8q). The posterior tissues on the 3D side were further divided into two bilateral lobes to make the embryo exhibit a pseudotwin phenotype (red arrows in fig. 8p'–q'). In a rare case, such a pseudotwin phenotype even developed duplicated larval shells (supplementary fig. S5k, Supplementary Material online). The remerged asymmetry in *L. goshimai* is reminiscent of the polarized development in the U0126-treated *Haliothis* embryos (Koop et al. 2007). These results indicate the existence of DV patterning regulators independent of *bmp2/4* or *chordin*. Accordingly, we retrieved a *bmp5–8* ortholog in *L. goshimai* (supplementary fig. S8, Supplementary Material online) and found that it showed asymmetric expression along the DV axis (Cui et al., unpublished data) (this may also explain the residual BMP signaling after *bmp2/4* knockdown).

The blastopore was also formed in 8-hpf embryos. Notably, we found that the blastopores were posteriorized in gene knockdown embryos (fig. 8g and m), showing sharp contrast with the normal blastopores formed ventrally (fig. 8a). This posteriorized blastopore was confirmed by *foxa* expression (fig. 8l and r, compared to fig. 8f). The blastopores of *L. goshimai* formed as a consequence of complicated morphogenetic events during gastrulation (fig. 6A). Thus, the

changes in blastopore location in these manipulated embryos support our speculation of altered morphogenetic changes after manipulating BMP signaling. To support this idea, we investigated the development of manipulated embryos using SEM. Since gene knockdown experiments could not provide sufficient embryos for SEM experiments, we analyzed the embryos treated with high-dose rhBMP4. In these embryos, although blastoporal tissues did not shrink into a small pore as in normal embryos, they were recognizable due to their adjacency to endodermal tissue and showed a comparable trend of posteriorization (supplementary fig. S6, Supplementary Material online). Thus, consistent to our speculation, these results did not reveal evident morphogenetic changes along the presumptive DV axis in the rhBMP4-treated embryos (supplementary fig. S6, Supplementary Material online).

Since posteriorized blastopores may have essential evolutionary implications, we sought to explore whether there was molecular evidence to indicate the developmental capacity of blastoporal cells, given that it was difficult to directly trace blastoporal development due to seriously disrupted development. Thus, we investigated the expression of *brachyury*. Although *brachyury* has been lost in some animal lineages, its expression in the blastoporal rim is highly similar in gastropod species (Lartillot, Lespinet et al. 2002; Koop et al. 2007; Perry et al. 2015). Specifically, normal *brachyury* expression of *L. goshimai* comprised three parts at 8 hpf (indicated by

numbers in [fig. 8s and t](#)): (1) the posterior rim of the blastopore, which showed a V shape and would contribute to the formation of the larval mouth; (2) the ventral midline; and (3) posterior expression with undetermined fates. We found that in both *bmp2/4*- and *chordin*-knockdown embryos, although *brachyury* expression changed considerably, a V-shaped expression pattern was still discriminable in blastoporal cells (number “1” in [fig. 8u and v](#)). This result indicated that despite the posteriorized localizations, the blastoporal cells seemed to still retain the developmental potential of the larval mouth in the knockdown embryos.

### Effects of BMP Signaling on Neurogenesis

We finally investigated neurogenesis after gene knockdown, given that the inhibitory effect of BMP signaling on neurogenesis has been suggested to be conserved in most animals ([Mizutani and Bier 2008](#)), but an opposite effect (in pretrochal tissues) is suggested in the mollusk *Ilyanassa* ([Lambert et al. 2016](#)). Distributions of two neural markers (5-HT and FMRamide), as well as the expression of two marker genes, namely, *pax6* (as in *Ilyanassa*; [Lambert et al. 2016](#)) and *elav* (a possibly universal neuron marker; [Pascale et al. 2008](#)), were explored.

The results did not reveal whether BMP signaling promoted or inhibited these neural markers in most cases ([fig. 9](#)). The only exception was 5-HT immunoactivity in the pretrochal region, which was undetectable after *bmp2/4* knockdown ([fig. 9e](#)) and generally enhanced after *chordin* knockdown ([fig. 9f](#)). These results indicated that neural tissues containing 5-HT were promoted by BMP signaling, which, however, seemed to be restricted to the pretrochal region (no 5-HT-containing neural tissues were recognized in the posttrochal regions of manipulated larvae). Another line of supportive evidence is that expanded pretrochal *pax6* expression could be observed in some *chordin*-knockdown larvae (the arrow in [fig. 9l](#)). This result is consistent with the positive role of BMP signaling in neurogenesis in the pretrochal region of *Ilyanassa* larvae ([Lambert et al. 2016](#)).

While investigations of larval stages did not reveal whether BMP signaling would promote or inhibit neurogenesis, we further explored whether the conserved roles of BMP signaling in neurogenesis might be detectable only in the early phase of neurogenesis ([Lambert et al. 2016](#)). The expression of *soxb* in the early gastrula at 4 hpf was analyzed, given that this stage may include processes of early neurogenesis, such as the definition of the neuroectoderm and commitment of neural stem cells, and that *soxb* is suggested to play essential roles in the early phase of neurogenesis ([Hartenstein and Stollewerk 2015](#)). However, it is also difficult to conclude whether *soxb* expression was inhibited or promoted in any group ([supplementary fig. S7B, Supplementary Material online](#)).

Instead of indicating positive or inhibitory effects, our results seemed to indicate that BMP signaling affected the organization of the nervous system. As revealed by FMRamide- or 5-HT-containing tissues, as well as both *pax6* and *elav* expression, a common phenotype after *bmp2/4* or *chordin* knockdown was the loss of featured

bilaterally distributed neural tissues ([fig. 9](#)). In accordance, we found that although *soxb* expression (at 6 hpf) showed a fully radial pattern under high-dose rhBMP4 treatment ([fig. 7x' and x''](#)), a bilateral pattern was restored in a portion of embryos when the treatment was weaker ([supplementary fig. S2m' and n', Supplementary Material online](#)).

## Discussion

While the DV patterning mechanism is considered conserved across bilaterian clades ([Bier and De Robertis 2015](#)), investigations of several spiralian representatives have revealed different results ([fig. 1a](#)). Moreover, in various spiralian phyla, DV patterning is deeply integrated into a highly specialized organizer-driven developmental mode ([Henry and Martindale 1999; Hejnal 2010; Lambert 2010; Nielsen 2010; Henry 2014](#)), with the underlying molecular mechanism largely unknown. Together, these two lines of evidence indicate that spiralian DV patterning is essential to explore the conservation and plasticity of animal DV patterning and to decipher the molecular network underlying the spiralian D-quadrant organizer.

In the present study, we explored the DV patterning of the mollusk *L. goshimai*; the major findings are presented in [figure 10](#). Our results suggest that under the regulation of the D-quadrant organizer, a *bmp2/4*-*chordin*-based molecular network determined the BMP signaling gradient in very early embryos (approximately 60-cell stage, [fig. 10a](#)). This gradient reflects the involvement of BMP signaling in DV patterning; early embryonic development was radialized when it was eliminated due to knockdown of *bmp2/4* or *chordin* ([fig. 10b](#)). Examinations of manipulated embryos further revealed alternations in the behavior of blastopore and the organization of the larval nervous system ([fig. 10b](#)). These results suggest connections of these two bilaterian-featured processes ([Martindale and Hejnal 2009; Nielsen 2012; Arendt et al. 2016; Nielsen 2018; Nielsen et al. 2018](#)) and DV patterning; and this may help to understand the evolution of the bilaterian body plans. The reemerged asymmetry additionally indicated undetermined factors regulating polarized development along the 3B–3D axis that were independent of *bmp2/4* or *chordin* ([fig. 10b](#)).

### *L. goshimai* DV Patterning Relies on *bmp2/4* and *chordin*

#### A Spiralian Case with DV Patterning Relying on BMP2/4 and Chordin

A major issue in the studies of spiralian DV patterning is that researchers have reported very different results using different systems ([fig. 1a](#)). Therefore, a paradox arises: while it is widely accepted that the common ancestor of bilaterians utilizes *bmp2/4* and *chordin* for DV patterning ([Bier and De Robertis 2015](#)), this character is not revealed in various spiralian representatives. Here, we revealed the DV patterning mechanism depending on *bmp2/4* and *chordin* in the mollusk *L. goshimai* by showing radialized development after *bmp2/4* or *chordin* knockdown, which was highly similar to the phenotype after organizer inhibition ([figs. 3 and 7](#)). This

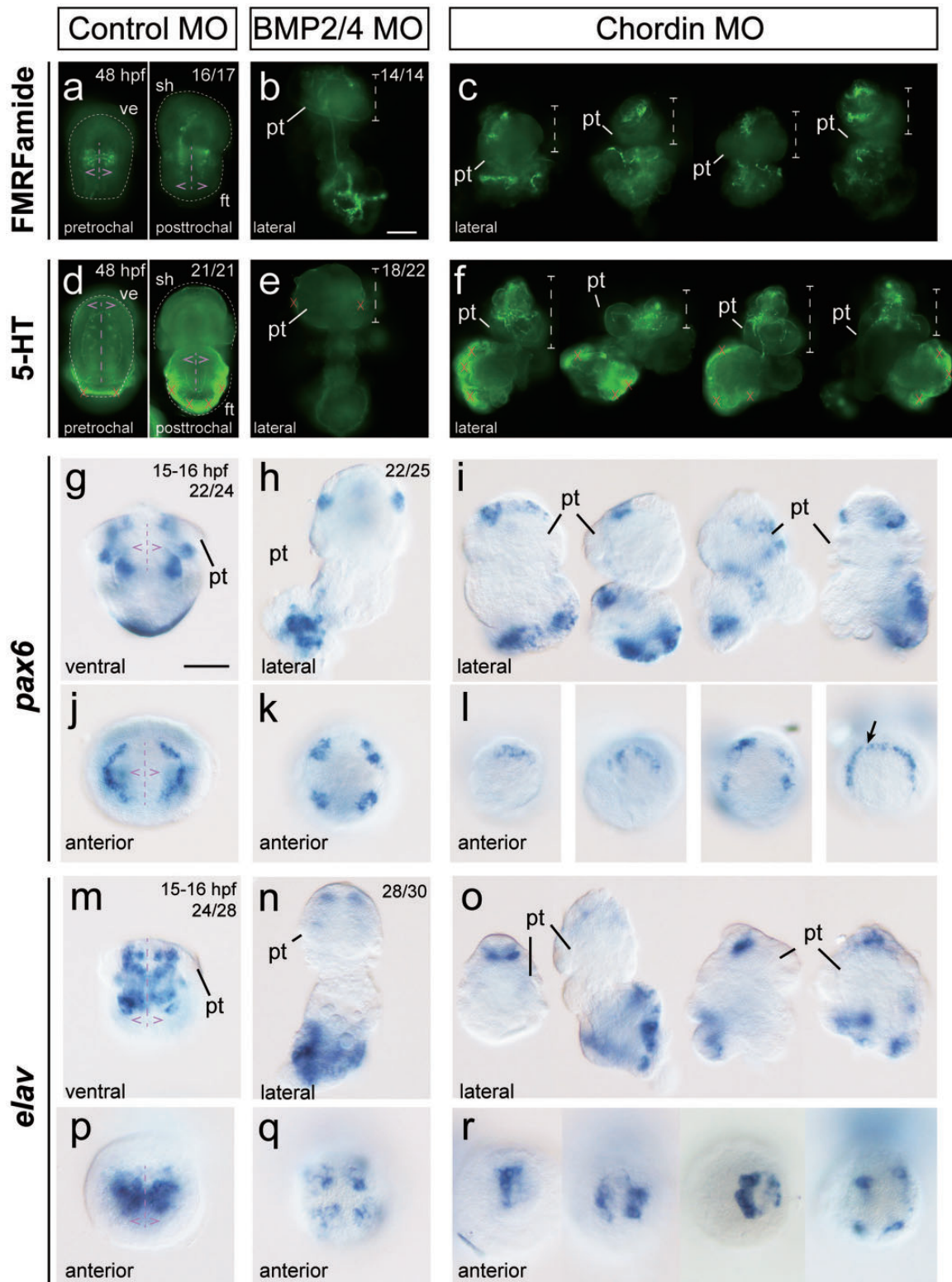


**FIG. 9.** Effects of BMP signaling on neurogenesis. The distributions of the neural markers FMRFamide and 5-HT, as well as expression of the neural marker genes *pax6* and *elav*, were investigated. Panels (a) and (d) show anterior views at two different focal planes (see more information in [supplementary fig. S7A, Supplementary Material online](#)) and (b) and (c) and (e) and (f) show lateral views with anterior to the top. The white dashed lines in (a) and (d) outline the velum (ve), shell (sh), and foot (ft) of control larvae, and for manipulated larvae (b, c, e, and f), they mark the pretrochal (head) region. In control embryos, the neural tissues in the larval head and foot indicated by the markers show ideal bilateral organizations (indicated by purple arrowheads). Since the larvae after *chordin* knockdown show relatively high levels of heterogeneity, representative larval phenotypes are provided (c, f, i, l, o, and r), and it is not possible to provide the number of individuals. Pretrochal *pax6* expression shows expansion in some larvae (the arrow in l). The red crosses in (d)–(f) indicate staining in cells that were not likely neural tissues given the lack of neurites. pt, prototroch. The bars represent 50  $\mu\text{m}$ .

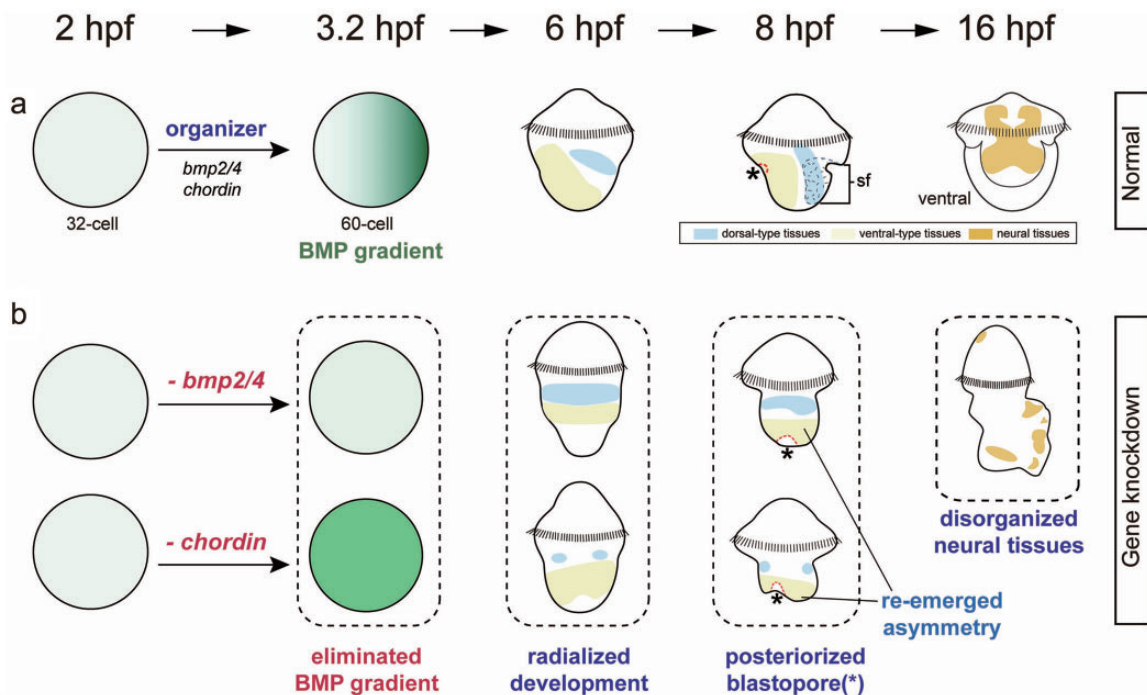


**FIG. 10.** Schematic diagram showing the major findings of the present study. Focusing on *bmp2/4* and *chordin*, we revealed the roles of the two genes (i.e., BMP signaling) in organizer function (fig. 5) and DV patterning of the mollusk *L. goshimai* (fig. 7). A close examination of the manipulated embryos revealed evidence showing the correlation between the BMP signaling gradient and the behavior of blastopores (fig. 8) and likely the organization of neural tissues (fig. 9). Unexpected asymmetrical development reemerged in the impaired embryos (fig. 8). See more information in the text.

result thus reveals a spiralian case retaining this conserved DV patterning mechanism, which has been indicated but not revealed for a long time. In the context of diverse reports in spiralian, the case of *L. goshimai* conversely represents an unusual example. For other mollusks, a similar mechanism may be expected in *Ilyanassa* and *Crassostrea*, given that current knowledge fits with a *bmp2/4-chordin*-based DV patterning framework (Lambert et al. 2016; Tan et al. 2017; Tan et al. 2018). Nevertheless, due to the very different experimental designs (see below), we could not determine to what degree the differences between our conclusion and that in the gastropod *Crepidula* (Lyons et al. 2020) would be explained by interspecies variations and differences in experimental strategies.

#### Insights into the Suggested Diversity of Spiralian DV Patterning Mechanisms

The different reports in spiralian DV patterning undoubtedly suggest the diversity of the underlying mechanisms. However, it is notable that the experimental designs of these studies vary in many aspects: strategies to influence BMP signaling (MOs, small molecule inhibitors, exogenous BMP proteins), indicators of DV patterning (cell lineages, characteristic tissues, marker gene expression), and the developmental stages investigated (early embryos, larvae) (Orii and Watanabe 2007; Kuo and Weisblat 2011; Lambert et al. 2016; Lanza and Seaver 2018, 2020a, 2020b; Lyons et al. 2020; Webster et al. 2021). Our results suggest that many of these factors would affect the

results and may contribute to the differences in the conclusions.

One of our major findings is that the developmental stages investigated would be essential for interpretations of the manipulated phenotypes. In *L. goshimai*, even though the developmental polarity was largely eliminated in early knockdown embryos (at 6 hpf, fig. 7), asymmetrical development could reemerge later (at 8 hpf, fig. 8). Later, larvae even exhibited a considerable degree of heterogeneity (fig. 3), and it was difficult to interpret whether and how DV patterning was changed in the larvae. These results indicate that the effects on DV patterning may be underestimated if only a few or too late developmental stages are analyzed.

Another difference among current studies is how researchers assess whether/how DV patterning is influenced. While cell lineage analysis has been particularly useful in studying spiralian development (Lambert 2010; Henry 2014; Seaver 2014), the gene expression data could also provide essential information (Martín-Durán et al. 2016). Therefore, multiple approaches, including both cell lineage analysis and gene expression analysis, may provide a more comprehensive interpretation of the phenotypes of manipulated embryos.

The manners employed to influence BMP signaling are also essential. Given the extreme complexity of BMP signaling that includes multiple ligands and antagonists and is under tight temporal and spatial regulations (Massagué 1998; Wu and Hill 2009), manipulations of different nodes of the pathway could cause varied BMP signaling levels and different biological results. Indeed, we showed that the phenotypes after

*chordin* knockdown and rhBMP4 treatment somewhat differentiated from each other. Although they both caused enhanced BMP signaling and produced radialized gene expression, *chordin* knockdown caused circular *soxb* expression (fig. 7s’), and fourfold symmetrical *soxb* expression was observed after high-dose rhBMP4 treatment (fig. 7x’). These differences could be caused by nodes of the signaling that were manipulated. The manipulated phenotypes of eye development also support the idea that the varied manners of manipulations on BMP signaling could generate different biological effects. We obtained a rather complicated scenario of eye development after different manipulations in *L. goshimai*. No eye formed after *bmp2/4* knockdown or high-dose rhBMP4 treatment; and generally extra eyes formed after *chordin* knockdown, or treatments of U0126 or low-dose rhBMP4 (fig. 3). Given that the different doses of rhBMP4 treatment produced no or extra eyes, these results indicate that in spiralian embryos, eye specification may require some appropriate level of BMP signaling in the head, and that much more or much less activity than normal blocks eye specification, while subtler manipulations can generate ectopic eyes. This may account for the inconsistent eye phenotypes when inhibiting organizer formation in different mollusks (no eye in *Ilyanassa* and extra eyes in *Tectura*; Lambert and Nagy 2001; Lambert and Nagy 2003) as well as the diverse biological effects detected after treatments of BMP proteins in different spiralian species (e.g., in *Crepidula*, *Ilyanassa*, and *Lottia*) (Lambert et al. 2016; Lyons et al. 2020; and this study).

## The Developmental Mode in Spiralian: Organizer Function and Other Aspects

### Relationships between the D-Quadrant Organizer and *bmp2/4* and *chordin*

A key characteristic of spiralian development is the D-quadrant organizer (Henry 2014). The underlying molecular mechanisms of organizer function have received much attention but remain largely unknown. Although MAPK signaling is essential in organizer function (Lambert and Nagy 2001; Lambert and Nagy 2003), the involved molecules are poorly understood. Demonstration of the involvement of *bmp2/4* in *Ilyanassa* organizer function represents key progress toward an in-depth understanding of spiralian organizers (Lambert et al. 2016). Here, our results suggest that *bmp2/4* may play similar roles in *L. goshimai*, an equal cleaver, as its ortholog in the unequal cleaver *Ilyanassa* (note the uncertainty that the activation of BMP2/4 may also be independent of the organizer; see fig. 5). Although the manners of organizer activation and MAPK signaling dynamics would differ significantly between the two types of embryos (Lambert and Nagy 2001; Lambert and Nagy 2003), the possibly consistent employment of *bmp2/4* suggests a conserved molecular network underlying the organizer function. Moreover, we showed that the establishment of the BMP signaling gradient in *L. goshimai* required *chordin* that was under the regulation of the organizer, supporting our speculation of the indispensable role of *chordin* in organizer function. Together, our hypothesis suggests that the canonical DV patterning molecular

network has been deeply integrated into the organizer function in spiralian development, thus consolidating the link between a highly clade-specific character (a D-quadrant organizer) and a conserved biological process (DV patterning; Lambert et al. 2016).

This hypothesis can be tested in more spiralian lineages, which would be important to understand the unique developmental mode in spiralian (Henry 2002; Henry 2014; Seaver 2016). Nevertheless, it is too soon to conclude that the involvement of BMP signaling in D-quadrant organizer signaling is conserved in spiralian or even mollusks, because BMP signaling has been suggested not to mediate organizer signaling in two annelids and a mollusk (Lanza and Seaver 2018, 2020a; Lyons et al. 2020; Webster et al. 2021). Similarly, although BMP signaling may regulate DV patterning (specification of neuroectoderm) of the annelid *Platynereis dumerilii* (Denes et al. 2007), current evidence is not sufficient to infer whether it mediates organizer signaling (the research focused on later organogenesis/neural patterning stages).

### Radialized Development in Early Embryos: Loss of the DV Axis

We found that the manipulations of DV patterning in *L. goshimai* caused radialized development in the gastrula (fig. 7). This phenotype was confirmed to be the result of loss of the DV axis given that it was also observed after inhibiting organizer function, a long-accepted manipulation to eliminate DV patterning in spiralian embryos (Guerrier et al. 1978; van den Biggelaar and Guerrier 1979; Martindale et al. 1985; Kühtreiber et al. 1988). We noticed that the radial gene expression patterns highly resembled those in earlier normal embryos (4.3 or 5 hpf), indicating that the radialized development may attribute to the altered morphogenetic changes during gastrulation/DV patterning. Indeed, previous studies have revealed that manipulations on organizer signaling cause misspecifications of widespread blastomeres before gastrulation (Guerrier et al. 1978; van den Biggelaar and Guerrier 1979; Martindale et al. 1985). Given that different cell clones of molluscan embryos can show distinct morphogenetic behaviors during gastrulation (Lyons et al. 2015), misspecifications of early blastomeres may result in altered behaviors and changed cell fates during gastrulation, which should account for the impaired DV patterning. However, current knowledge on the normal DV patterning process of *L. goshimai* is limited, for example, how each blastomere is specified at the onset of gastrulation and how each blastomere further differentiates and behaves during gastrulation. The lack of these data prevents implying the details regarding how the radialized phenotype was developed; this issue may be addressed by further investigations to reveal more details of the normal DV patterning process. They may also help to explain the apparent differences between the radialized phenotype in *L. goshimai* and the dorsalization/ventralization phenotypes that have been frequently observed in other animals, which refer to compensatory expansion and reduction of dorsal-/ventral-type tissues after interfering with DV patterning (Sasai et al. 1994; François and Bier 1995; Lowe et al. 2006; Lapraz et al. 2009).

Although radialized development was the major effect after manipulation of BMP signaling, we did detect evidence indicating limited dorsal/ventralization. We found the midline *brachyury* expression was lost when *bmp2/4* was inhibited (fig. 8v) but not when *chordin* was knocked down (fig. 8u). In *Patella*, the midline tissues expressing *brachyury* are derived from 2d blastomeres that are distributed dorsally in early embryos (e.g., at the 60-cell stage; Lartillot, Lespinet et al. 2002); and this could be expected in its close relative *L. goshimai*. Therefore, the loss of midline *brachyury* expression could be considered the loss of 2d blastomere specification. This is consistent with the previous analysis based on cleavage patterns (in early embryos) revealing the lack of dorsal-fate blastomeres after inhibiting organizer formation, that is, a trend of ventralization (Martindale et al. 1985). After *chordin* knockdown, the dorsal-most tissues would be unaffected; this explains the unchanged midline *brachyury* expression (on the 3D side) in the manipulated embryos (although the midline tissues are situated ventrally after gastrulation in normal embryos; see supplementary fig. S5, Supplementary Material online for the evidence of this morphogenetic change).

#### Reemerged Asymmetry in the Late Embryo

Despite the radialized development in 6-hpf embryos, we detected asymmetry along the 3B–3D axis in the 8-hpf *chordin*-knockdown embryos (fig. 8). Although we do not deny the possibility of incomplete knockdown of gene function, late asymmetric development may be related to cellular asymmetry detectable as early as the 60-cell stage (fig. 2b), which was not affected by gene knockdown (fig. 5Ac–Ae; note the different sizes of  $3a^2/b^2$  and  $3c^2/d^2$ ). This asymmetry may directly determine lineage-specific, asymmetrical cell specifications on the 3B and 3D sides, or it may generate asymmetrical expression of other DV patterning genes (e.g., *bmp5–8*, *tolloid*) that may somewhat restore interrupted DV patterning. In any case, this phenomenon may reflect the profound effect of the stereotype cleavage pattern in regulating DV patterning. A latent DV axis independent of the organizer is also noticed in *Haliotis* (Koop et al. 2007). These potential DV patterning regulators are warrant of further investigations.

## Materials and Methods

### Animals

Adults of *L. goshimai* Nakayama, Sasaki, and Nakano, 2017 were collected from intertidal rocks in Qingdao, China. Spawning occurred after collection during the reproductive season (from June to August). During other seasons, algae were scraped from the surfaces of rocks inhabited by the limpets and cultured on plastic sheets under constant light. At 18–22°C, the limpets fed these cultured algae could become sexually mature in several weeks. On some occasions, spawning was induced through elevated temperature, drying, rigorous water flow, or sperm suspensions. The adult limpets were allowed to spawn in separate 100-mL cups, and the

gametes were collected. Artificial fertilization was performed by mixing sperm and oocyte suspensions.

Fertilized eggs were incubated in filtered seawater (FSW) containing antibiotics (100 unit/mL benzylpenicillin and 200 µg/mL streptomycin sulfate) in an incubator at 25°C. The units of all developmental stages are in hpf except for the very early developmental stages (before the 64-cell stage). For in situ hybridization (ISH), samples at the desired developmental stages were fixed in 4% paraformaldehyde (1× PBS, 100 mM EDTA, and 0.1% Tween-20, pH 7.4), transferred to methanol, and stored at –20°C until use. Older larvae (after 15 hpf) were anesthetized with 0.1% sodium azide or 125 mM magnesium chloride before fixation. Analyses of the samples were performed as previously described, including ISH (Huan et al. 2020), phalloidin staining (Kurita et al. 2009), and scanning electron microscopy (SEM; Tan et al. 2017).

### pSmad1/5/8 Staining and Quantification

A primary antibody from Cell Signaling Technology (Cat. No. 138205) was used to detect pSmad1/5/8 activities in *L. goshimai*. Immunostaining was performed as previously described (Lapraz et al. 2009). The pSmad1/5/8 signals in 12 blastomeres at the animal pole were quantified by normalization to the background fluorescence and they were used to estimate the differences in pSmad1/5/8 activities between different groups. For control embryos, these blastomeres were divided into D- and B-side groups based on their very different signal levels, and all investigated blastomeres of the manipulated embryos were considered a single group given similar signal intensities (the inserts in fig. 5Ao and supplementary fig. S1e–o, Supplementary Material online). Statistical analyses were performed using one-way ANOVA, and a significance threshold of 0.05 was used. A detailed procedure is provided in the supplementary text, Supplementary Material online and supplementary fig. S1, Supplementary Material online.

### Genes and MOs

*L. goshimai* gene sequences were retrieved from a developmental transcriptome that we developed previously (Huan et al. 2020) (supplementary figs. S8–S12, Supplementary Material online). Translation-blocking MOs targeting *bmp2/4* (BMP2/4 MO1) and *chordin* (Chordin MO1), as well as a negative control MO (a mutated Chordin MO [control MO1]), were used. We also used other nonoverlapping specific MOs (BMP2/4 MO2 and Chordin MO2), as well as a standard MO (control MO2), and we confirmed that they generated similar effects to the aforementioned MOs. Details of the MOs are provided in the supplementary text, Supplementary Material online.

### MO Microinjection

Microinjection was performed using a micromanipulator. The injection solutions contained 0.05% phenol red, 500 ng/µL FITC-conjugated dextran, and 0.25 mM MO. No more than 1.5% of the oocyte volume of the injection solution was injected into the unfertilized oocytes (estimated by the diameter of the injected solution). After fertilization, successful



injections were confirmed by the presence of green fluorescence inside the cells; embryos that exhibited no fluorescence were removed. In trials aiming to explore pSmad1/5/8 distribution, FITC-conjugated dextran was excluded from the injection solution to avoid causing relatively high background values in subsequent immunostaining. On these occasions, the injections were performed slowly and carefully to ensure that every injection was successful.

### Treatments with U0126 or rhBMP4

U0126 and rhBMP4 treatment experiments were performed in 12-well plates. U0126 (75  $\mu$ M) treatment was performed between the 16- and 64-cell stages, and rhBMP4 treatment was performed between 0 and 6 hpf. Two concentrations of rhBMP4 were used, including 0.5  $\mu$ g/mL (high-dose treatment) and 0.075  $\mu$ g/mL (low-dose treatment). After treatment, the embryos were fixed for further analyses or washed with FSW and allowed to develop to the desired developmental stages. A detailed procedure is provided in the [supplementary text, Supplementary Material online](#).

Oocytes from at least three females were used in every assay involving rhBMP4/U0126 treatment or MO injection (ISH, immunostaining, eye number investigation, and SEM), and we confirmed that maternal effects did not evidently influence the outcomes of most experiments (see [supplementary text, Supplementary Material online](#) for the limited maternal effects in the low-dose rhBMP4 treatment group).

### Imaging

Images were recorded using a Nikon 80i microscope. The contrast and brightness of the images were adjusted using Photoshop software; when performed, such adjustments were applied to the whole image rather than to any particular region.

### Supplementary Material

[Supplementary data](#) are available at *Molecular Biology and Evolution* online.

### Acknowledgments

The authors are grateful to Dian-Han Kuo for engaging in thoughtful discussions throughout the course of the study and for critically revising the draft. The authors thank Dehui Sun, Menglu Cui, and Xinyu Liu for performing some ISH and immunostaining experiments, Bo Dong and Grigory Genikhovich for their discussions and comments on the draft, Ferdinand Marlétaz for providing the assembled transcriptomic data of various spiralian and for the helpful discussions, and Patrick Müller, Ulrich Technau, and Lingyu Wang for their helpful discussions. The authors thank the three anonymous reviewers for thoughtful suggestions. This work was supported by the National Key R&D Program of China (grant number 2018YFD0900104); the Marine S&T Fund of Shandong Province for Pilot National Laboratory for Marine Science and Technology (Qingdao) (grant number 2018SDKJ0302-1); the China Agriculture Research System (grant number CARS-49); the National Natural Science Foundation of China (grant numbers 42076123, 31472265

and 41776157); the Youth Innovation Promotion Association CAS (grant number 2018239); and the Taishan Scholar Project Fund of Shandong Province of China (grant number tsqn202103129).

### Data Availability

The sequences of *Lottia goshimai* genes used in this work are deposited in GenBank with accession numbers MN528131 (*bmp2/4*), MN528132 (*bmp5-8*), MN528133 (*chordin*), MZ822425 (*chordin-like*), MN528139 (*brachyury*), MN528140 (*gata2/3*), MN528141 (*pax6*), MN528142 (*foxa*), and MZ822426 (*hsp90a*).

### References

- Akiyama-Oda Y, Oda H. 2006. Axis specification in the spider embryo: *dpp* is required for radial-to-axial symmetry transformation and *sog* for ventral patterning. *Development*. 133(12):2347–2357.
- Anderson DT. 1969. On the embryology of the cirripede crustaceans *Tetraclita rosea* (Krauss), *Tetraclita purpurascens* (Wood), *Chthamalus antennatus* (Darwin) and *Chamaesipho columna* (Spengler) and some considerations of crustacean phylogenetic relationships. *Phil Trans R Soc Lond B Biol Sci*. 256:183–235.
- Arendt D, Tosches MA, Marlow H. 2016. From nerve net to nerve ring, nerve cord and brain—evolution of the nervous system. *Nat Rev Neurosci*. 17(1):61–72.
- Bier E, De Robertis EM. 2015. BMP gradients: a paradigm for morphogen-mediated developmental patterning. *Science*. 348(6242):aaa5838.
- Clement AC. 1962. Development of *Ilyanassa* following removal of the D macromere at successive cleavage stages. *J Exp Zool*. 149(3):193–215.
- Denes AS, Jékely G, Steinmetz PRH, Raible F, Snyman H, Prud'homme B, Ferrier DEK, Balavoine G, Arendt D. 2007. Molecular architecture of annelid nerve cord supports common origin of nervous system centralization in Bilateria. *Cell*. 129(2):277–288.
- DuBuc TQ, Ryan JF, Martindale MQ. 2019. “Dorsal–ventral” genes are part of an ancient axial patterning system: evidence from *Trichoplax adhaerens* (Placozoa). *Mol Biol Evol*. 36(5):966–973.
- Erwin DH. 2009. Early origin of the bilaterian developmental toolkit. *Philos Trans R Soc Lond B Biol Sci*. 364(1527):2253–2261.
- François V, Bier E. 1995. *Xenopus chordin* and *Drosophila short gastrulation* genes encode homologous proteins functioning in dorsal–ventral axis formation. *Cell*. 80(1):19–20.
- García Abreu J, Coffinier C, Larraín J, Oelgeschläger M, De Robertis EM. 2002. Chordin-like CR domains and the regulation of evolutionarily conserved extracellular signaling systems. *Gene*. 287(1–2):39–47.
- Genikhovich G, Fried P, Prunster MM, Schinko JB, Gilles AF, Fredman D, Meier K, Iber D, Technau U. 2015. Axis patterning by BMPs: cnidarian network reveals evolutionary constraints. *Cell Rep*. 10(10):1646–1654.
- Guerrier P, van den Biggelaar JA, van Dongen CA, Verdonk NH. 1978. Significance of the polar lobe for the determination of dorsoventral polarity in *Dentalium vulgare* (da Costa). *Develop Biol*. 63(1):233–242.
- Guignard L, Fiúza U-M, Leggio B, Laussu J, Faure E, Michelin G, Biasuz K, Hufnagel L, Malandain G, Godin C, et al. 2020. Contact area–dependent cell communication and the morphological invariance of ascidian embryogenesis. *Science*. 369(6500):pii: 369/6500/eaar5663.
- Hartenstein V, Stollewerk A. 2015. The evolution of early neurogenesis. *Dev Cell*. 32(4):390–407.
- Hejnal A. 2010. A twist in time—the evolution of spiral cleavage in the light of animal phylogeny. *Integr Comp Biol*. 50(5):695–706.
- Henry JJ. 2002. Conserved mechanism of dorsoventral axis determination in equal-cleaving spiralian. *Dev Biol*. 248(2):343–355.
- Henry JJ, Martindale MQ. 1999. Conservation and innovation in spiralian development. *Hydrobiologia*. 402:255–265.

- Henry JJ, Perry KJ. 2008. MAPK activation and the specification of the D quadrant in the gastropod mollusc, *Crepidula fornicata*. *Dev Biol*. 313(1):181–195.
- Henry JQ. 2014. Spiralian model systems. *Int J Dev Biol*. 58(6–8):389–401.
- Huan P, Wang Q, Tan S, Liu B. 2020. Dorsoventral decoupling of Hox gene expression underpins the diversification of molluscs. *Proc Natl Acad Sci U S A*. 117(1):503–512.
- Kenny NJ, Namigai EKO, Dearden PK, Hui JHL, Grande C, Shimeld SM. 2014. The Lophotrochozoan TGF- $\beta$  signalling cassette—diversification and conservation in a key signalling pathway. *Int J Dev Biol*. 58(6–8):533–549.
- Koop D, Richards GS, Wanninger A, Gunter HM, Degnan BM. 2007. The role of MAPK signaling in patterning and establishing axial symmetry in the gastropod *Haliotis asinina*. *Dev Biol*. 311(1):200–212.
- Kühtreiber WM, Til EH, Dongen CAM. 1988. Monensin interferes with the determination of the mesodermal cell line in embryos of *Patella vulgata*. *Roux Arch Dev Biol*. 197(1):10–18.
- Kuo D-H, Weisblat DA. 2011. A new molecular logic for BMP-mediated dorsoventral patterning in the leech *Helobdella*. *Curr Biol*. 21(15):1282–1288.
- Kurita Y, Deguchi R, Wada H. 2009. Early development and cleavage pattern of the Japanese purple mussel, *Septifer virgatus*. *Zoolog Sci*. 26(12):814–820.
- Lambert JD. 2010. Developmental patterns in spiralian embryos. *Curr Biol*. 20(2):R72–R77.
- Lambert JD, Johnson AB, Hudson CN, Chan A. 2016. Dpp/BMP2-4 mediates signaling from the D-quadrant organizer in a Spiralian embryo. *Curr Biol*. 26(15):2003–2010.
- Lambert JD, Nagy LM. 2003. The MAPK cascade in equally cleaving spiralian embryos. *Dev Biol*. 263(2):231–241.
- Lambert JD, Nagy LM. 2001. MAPK signaling by the D quadrant embryonic organizer of the mollusc *Ilyanassa obsoleta*. *Development*. 128(1):45–56.
- Lanza AR, Seaver EC. 2020a. Activin/nodal signaling mediates dorsal-ventral axis formation before third quartet formation in embryos of the annelid *Chaetopterus pergamentaceus*. *Evodevo*. 11:17.
- Lanza AR, Seaver EC. 2020b. Functional evidence that activin/nodal signaling is required for establishing the dorsal-ventral axis in the annelid *Capitella teleta*. *Development*. 147(18):dev189373.
- Lanza AR, Seaver EC. 2018. An organizing role for the TGF- $\beta$  signaling pathway in axes formation of the annelid *Capitella teleta*. *Dev Biol*. 435(1):26–40.
- Lapraz F, Besnardeau L, Lepage T. 2009. Patterning of the dorsal-ventral axis in echinoderms: insights into the evolution of the BMP-Chordin signaling network. *PLoS Biol*. 7(11):e1000248.
- Lartillot N, Le Gouar M, Adoutte A. 2002. Expression patterns of *fork head* and *gooseoid* homologues in the mollusc *Patella vulgata* supports the ancestry of the anterior mesendoderm across Bilateria. *Dev Genes Evol*. 212(11):551–561.
- Lartillot N, Lespinet O, Vervoort M, Adoutte A. 2002. Expression pattern of *Brachyury* in the mollusc *Patella vulgata* suggests a conserved role in the establishment of the AP axis in Bilateria. *Development*. 129(6):1411–1421.
- Lemaire P, Smith WC, Nishida H. 2008. Ascidians and the plasticity of the chordate developmental program. *Curr Biol*. 18(14):R620–R631.
- Lowe CJ, Terasaki M, Wu M, Freeman RM, Runft L, Kwan K, Haigo S, Aronowicz J, Lander E, Gruber C, et al. 2006. Dorsoventral patterning in hemichordates: insights into early chordate evolution. *PLOS Biol*. 4(9):e291.
- Lyons DC, Henry JQ. 2014. Ins and outs of spiralian gastrulation. *Int J Dev Biol*. 58(6–8):413–428.
- Lyons DC, Perry KJ, Batzel G, Henry JQ. 2020. BMP signaling plays a role in anterior-neural/head development, but not organizer activity, in the gastropod *Crepidula fornicata*. *Dev Biol*. 463(2):135–157.
- Lyons DC, Perry KJ, Henry JQ. 2015. Spiralian gastrulation: germ layer formation, morphogenesis, and fate of the blastopore in the slipper snail *Crepidula fornicata*. *Evodevo*. 6:24.
- Martín-Durán JM, Passamanek YJ, Martindale MQ, Hejnol A. 2016. The developmental basis for the recurrent evolution of deuterostomy and protostomy. *Nat Ecol Evol*. 1(1):5–0005.
- Martindale MQ, Doe CQ, Morrill JB. 1985. The role of animal-vegetal interaction with respect to the determination of dorsoventral polarity in the equal-cleaving spiralian, *Lymnaea palustris*. *Wilhelm Roux' Archiv*. 194(5):281–295.
- Martindale MQ, Hejnol A. 2009. A developmental perspective: changes in the position of the blastopore during bilaterian evolution. *Dev Cell*. 17(2):162–174.
- Massagué J. 1998. TGF- $\beta$  signal transduction. *Annu Rev Biochem*. 67:753–791.
- Mizutani CM, Bier E. 2008. EvoD/Vo: the origins of BMP signalling in the neuroectoderm. *Nat Rev Genet*. 9(9):663–677.
- Nielsen C. 2012. How to make a protostome. *Invert Systemat*. 26(1):25–40.
- Nielsen C. 2018. Origin of the trochophora larva. *R Soc Open Sci*. 5(7):180042.
- Nielsen C. 2010. Some aspects of spiralian development. *Acta Zoologica*. 91(1):20–28.
- Nielsen C, Brunet T, Arendt D. 2018. Evolution of the bilaterian mouth and anus. *Nat Ecol Evol*. 2(9):1358–1376.
- Orii H, Watanabe K. 2007. Bone morphogenetic protein is required for dorso-ventral patterning in the planarian *Dugesia japonica*. *Dev Growth Differ*. 49(4):345–349.
- Pascale A, Amadio M, Quattrone A. 2008. Defining a neuron: neuronal ELAV proteins. *Cell Mol Life Sci*. 65(1):128–140.
- Patterson GI, Padgett RW. 2000. TGF beta-related pathways. roles in *Caenorhabditis elegans* development. *Trends Genet*. 16(1):27–33.
- Perry KJ, Lyons DC, Truchado-Garcia M, Fischer AHL, Helfrich LW, Johansson KB, Diamond JC, Grande C, Henry JQ. 2015. Deployment of regulatory genes during gastrulation and germ layer specification in a model spiralian mollusc *Crepidula*. *Dev Dyn*. 244(10):1215–1248.
- Saina M, Genikhovich G, Renfer E, Technau U. 2009. BMPs and Chordin regulate patterning of the directive axis in a sea anemone. *Proc Natl Acad Sci U S A*. 106(44):18592–18597.
- Sasai Y, Lu B, Steinbeisser H, Geissert D, Gont LK, De Robertis EM. 1994. *Xenopus chordin*: a novel dorsalizing factor activated by organizer-specific homeobox genes. *Cell*. 79(5):779–790.
- Seaver EC. 2016. Annelid models I: *capitella teleta*. *Curr Opin Genet Dev*. 39:35–41.
- Seaver EC. 2014. Variation in spiralian development: insights from polychaetes. *Int J Dev Biol*. 58(6–8):457–467.
- Tan S, Huan P, Liu B. 2017. Expression patterns indicate that BMP2/4 and Chordin, not BMP5-8 and gremlin, mediate dorsal-ventral patterning in the mollusk *Crassostrea gigas*. *Dev Genes Evol*. 227(2):75–84.
- Tan S, Huan P, Liu B. 2018. An investigation of oyster TGF- $\beta$  receptor genes and their potential roles in early molluscan development. *Gene*. 663:65–71.
- van den Biggelaar JA, Guerrier P. 1979. Dorsoventral polarity and mesentoblast determination as concomitant results of cellular interactions in the mollusk *Patella vulgata*. *Dev Biol*. 68(2):462–471.
- van den Biggelaar JAM. 1977. Development of dorsoventral polarity and mesentoblast determination in *Patella vulgata*. *J Morphol*. 154(1):157–186.
- Van der Zee M, Stockhammer O, von Levetzow C, Nunes da Fonseca R, Roth S. 2006. Sog/Chordin is required for ventral-to-dorsal Dpp/BMP transport and head formation in a short germ insect. *Proc Natl Acad Sci U S A*. 103(44):16307–16312.
- Wang YC, Ferguson EL. 2005. Spatial bistability of Dpp-receptor interactions during drosophila dorsal-ventral patterning. *Nature*. 434(7030):229–234.
- Webster NB, Corbet M, Sur A, Meyer NP. 2021. Role of BMP signaling during early development of the annelid *Capitella teleta*. *Dev Biol*. 478:183–204.
- Wu MY, Hill CS. 2009. TGF- $\beta$  superfamily signaling in embryonic development and homeostasis. *Dev Cell*. 16(3):329–343.